The total and updated lagrangian formulations of state-based peridynamics

Guy L. Bergel & Shaofan Li

Computational Mechanics
Solids, Fluids, Structures, Fluid-Structure Interactions, Biomechanics, Micromechanics, Multiscale Mechanics, Materials, Constitutive Modeling, Nonlinear Mechanics, Aerodynamics

ISSN 0178-7675

Comput Mech
DOI 10.1007/s00466-016-1297-8

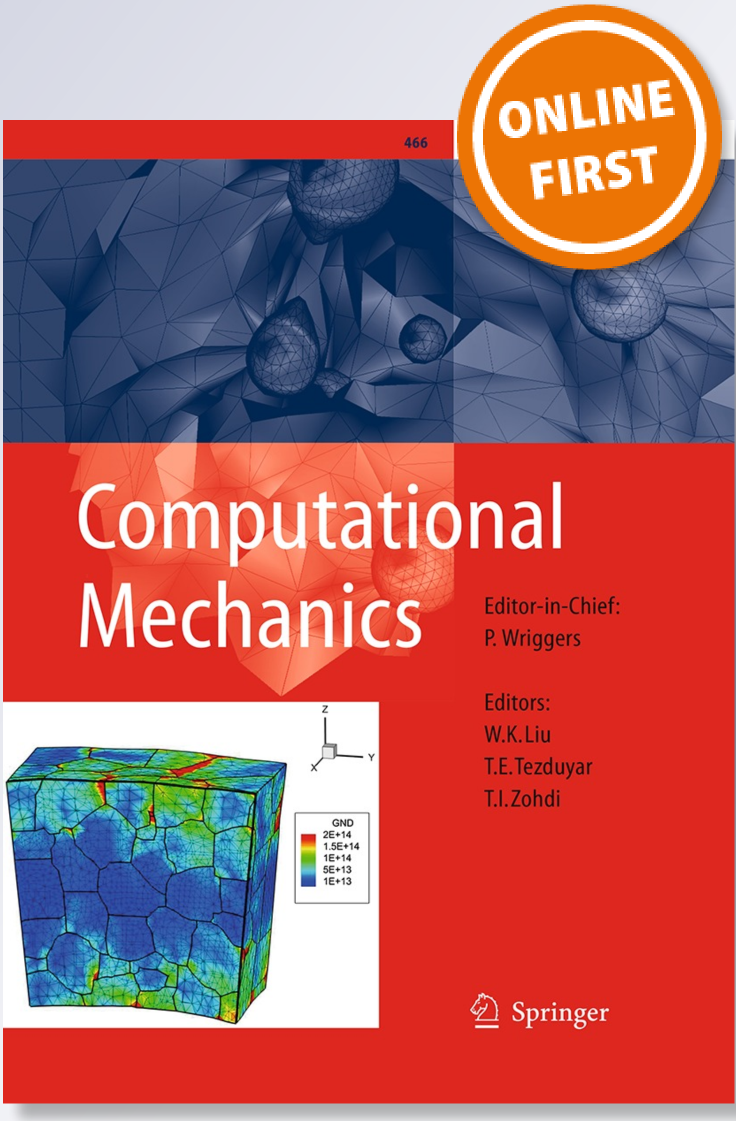

Springer

Comput Mech
DOI 10.1007/s00466-016-1297-8

ORIGINAL PAPER

The total and updated lagrangian formulations of state-based peridynamics

Guy L. Bergel[1] · Shaofan Li[1]

Received: 18 October 2015 / Accepted: 22 April 2016

Abstract The peridynamics theory is a reformulation of nonlocal continuum mechanics that incorporates material particle interactions at finite distances into the equation of motion. State-based peridynamics is an extension of the original bond-based peridynamics theory wherein the response of an individual particle depends collectively on its interaction with neighboring particles through the concept of state variables. In this paper, the more recent non-ordinary state-based Peridynamics formulations of both the total (referential) Lagrangian approach as well as the updated (spatial) Lagrangian approach are formulated. In doing so, relations of the state variables are defined through various nonlocal differential operators in both material and spatial configurations in the context of finite deformation. Moreover, these nonlocal differential operators are mathematically and numerically shown to converge to the local differential operators, and they are applied to derive new force states and deformation gradients.

Keywords Continuum mechanics · Deformation gradient · Finite elasticity · Nonlocal theory · State-based peridynamics · Updated Lagrangian

1 Introduction

Peridynamics is a nonlocal reformulation of continuum mechanics theory that was first developed in Silling [25]. The peridynamic equation of motion introduces a nonlocal integral operator that utilizes a pairwise force density to replace the stress divergence term in classical continuum mechanics. This force density relies on the stretch and initial positions of a network of particle bonds within the compact support of a given point in space, termed as the *horizon*. The nonlocal peridynamic equation of motion allows for singular displacement fields such as cracks to form spontaneously in portions of a given body where they did not previously exist.

A major shortcoming of the initial formulation of peridynamics (also termed bond-based peridynamics) is that each individual bond deforms independently based on a pair potential that can only describe the state of the two particles connecting to that bond. It was shown in Silling [25] that this shortcoming constrains the Lamé parameters λ and μ to be equal, which thus requires the Poisson ratio ν to be 0.25 in the case of linear isotropic elasticity. In Fact, Finnis and Sinclair [10] found that in molecular dynamics the pair potential based stress-strain relation can only produce an equilibrium solution if the two Lamé parameters λ and μ are identical, which is a special case (isotropic case) of the well-known Cauchy relation, e.g. [12]. In Silling et al. [26], an alternative version of peridynamics termed state-based peridynamics was developed using the concept of state variables, such as the force and deformation states. State variables are functions of the undeformed and deformed particle bonds that can describe non-linear and discontinuous fields in a horizon. Force states were introduced to replace the force density functions in the equation of motion. Moreover, [26] also introduced a specific form of the state-based theory, namely the non-ordinary state-based peridynamics, with force states that are derived directly from the principle of virtual work through constitutive relations of conventional continuum mechanics [31]. The force states in non-ordinary state-based peridynamics obtain their directionality through parameters such as stress, and they are not necessarily in parallel to the direction of a given bond that connects two

✉ Shaofan Li
shaofan@berkeley.edu

1 Department of Civil and Environmental Engineering, University of California, Berkeley, CA 94720, USA

Published online: 11 May 2016

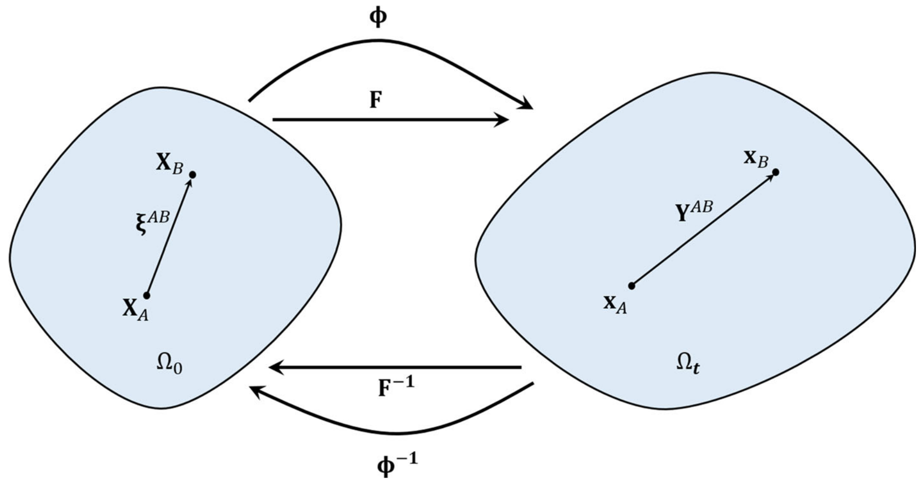

Fig. 1 Schematic illustration of the kinematics of finite deformation: The referential (material) configuration and the spatial (current) configuration, where $\boldsymbol{\Phi} : \Omega_0 \rightarrow \Omega_t$ is the motion and $\mathbf{F}$ is the deformation gradient

particles. Deformation states were also introduced in the general state-based peridynamics theory. In addition, a peridynamic deformation gradient was derived as a function of the collective deformation states within a given horizon in the referential configuration. The stress of a given point is defined by specified constitutive relations that are a function of the deformation gradient of its horizon.

In the subsequent developments of non-ordinary state-based peridynamics, the theory is extended and related to the stress divergence in continuum mechanics. For example, it is shown in Silling and Lehoucq [28] that the peridynamic equivalent of the first Piola-Kirchhoff stress tensor converges to the corresponding value of its counterpart in classical continuum mechanics as the horizon radius approaches zero, i.e. as the neighboring interactions of each particle become increasingly dense and localized. It has also been shown that in the same limit, the material divergence of the first Piola-Kirchhoff stress tensor also converges to its corresponding value in the equation of motion in classical continuum mechanics. In Silling and Lehoucq [29], several other aspects of the relation between state-based peridynamics and continuum mechanics were introduced. Examples include peridynamic balance laws, and constitutive relations, just to name a few.

The main objective of peridynamics is to resolve the discontinuity in field variables such as displacements (strong discontinuity) and temperature. Since its initial publication, peridynamics has been successfully implemented in various computer simulations to capture discontinuities such as fracture and crack propagation in solids, e.g. [1,5,6,11,13–15,20,27,30] among many others.

In actual material and structural failures, the material defects are always accompanied by finite deformations. The computational nonlinear continuum mechanics has two Lagrangian approaches in the context of finite deformation: the *Total Lagrangian* approach and the *Updated Lagrangian* approach. There approaches formulate the balance laws for a physical object according to the spatial domain that it is occupying, which corresponds to either a referential (material) configuration or a spatial (current) configuration respectively, as shown in Fig. 1. The current form of state-based peridynamics is formulated in the referential configuration only, and hence it is a total Lagrangian formulation. In the context Galerkin finite element method, one may find the detailed discussions on the updated Lagrangian method as well as the total Lagrangian method in the literature, e.g. [2,3]. In fact, both approaches, i.e. the updated Lagrangian formulation and the total Lagrangian formulation, have been extensively applied to solve nonlinear solid mechanics problems in nonlinear Galerkin finite element method. However, they are distinctively different approaches in meshfree particle methods. In fact, the current state-based peridynamics adopts the total Lagrangian appraoch; whereas both Molecular Dynamics and the Smoothed Particle Hydrodynamics (SPH) adopt the updated Lagrangian approach, which is essential to computational failure mechanics and computational fluid dynamics.

The main objective of this work is to extend the non-ordinary state-based peridynamics formulation of nonlocal continuum mechanics to include both referential (material) and spatial (current) descriptions in the context of finite deformations. In addition, we generalize the notion of the nonlocal derivative of non-ordinary state-based peridynamics by formulating various discrete nonlocal differential operators with respect to different configuration spaces.

In the next section, we briefly outline the concept of non-ordinary state-based peridynamics. In the third section, the nonlocal differential operators are introduced, and new force states and a deformation gradient are derived. We conclude the paper in Sect. 4 with a simple numerical example of elastic bar with a nonlinear uniaxial deformation to numerically illustrate the differences between the total Lagrangian approach and the update Lagrangian approach, and to study the convergence of the proposed nonlocal operators.

2 Non-ordinary state-based peridynamics

For a self-containedness of the presentation, we first review and outline non-ordinary state-based peridynamics, which is largely based on [29] and [22]. However, we adopt a slightly different definitions and terminologies.

Consider a reference domain $\Omega_0 \subset \mathbb{R}^d$ of dimension d composed of a discretized set of particles. Suppose each particle with reference position $\boldsymbol{X}^A \in \mathbb{R}^d$ is influenced by neighboring forces from other particles within a "sphere of influence" denoted as its *horizon* $\mathcal{H}^A$, with radius $\delta^A \in \mathbb{R}^+$. Each neighboring particle has a reference position $\boldsymbol{X}^B \in \mathbb{R}^d$, and forms a bond with particle A defined as

$$\boldsymbol{\xi}^{AB} := \boldsymbol{X}^B - \boldsymbol{X}^A, \quad \forall \quad \mathbf{X}^B \in \mathcal{H}^A$$

where A, B are particle indices.

Figure 2 illustrates the configuration of a peridynamic horizon and undeformed bonds. These bonds enable long-range particle interactions, even at finite distances. In addition, the *force state* and *deformation state* are defined as the energy conjugate pair that replaces the standard stress-strain approach of classical continuum mechanics. State variables are underlined and notated by indicating their point in space and time in brackets, and the variable that they map in angled brackets. Unlike their classical continuum mechanics counterparts, state variables in peridynamics have the ability to describe fields that are discontinuous across the horizon [26], thus providing a means of determining stresses and strains on the surface of a discontinuity, such as a crack.

The deformation state is defined as

$$\underline{\boldsymbol{Y}}^{AB}[\boldsymbol{x}^A, t]\langle\boldsymbol{\xi}^{AB}\rangle := \boldsymbol{x}(\boldsymbol{X}^B, t) - \boldsymbol{x}(\boldsymbol{X}^A, t), \quad \forall \ \mathbf{X}^B \in \mathcal{H}^A, \tag{1}$$

which is the relative position vector of the two particles in the current configuration. Each individual vector of the deformation state is called the deformed bond vector. The deformation state at a given point describes the current configuration of the horizon of particle A based on the interaction with its neighboring particles. By standard convention in continuum mechanics, the lowercase position vectors are used to indicate the position vectors in the current configuration of the deformed domain, Ω; whereas the uppercase position vectors are used to indicate the position vectors in the referential configuration of the undeformed domain, Ω_0.

These spatial positions, notated as $\boldsymbol{x}^A := \boldsymbol{x}(\boldsymbol{X}^A, t)$, $\boldsymbol{x}^B := \boldsymbol{x}(\boldsymbol{X}^B, t)$ are both a function of time and the reference position. These dependent variables will be assumed for the remainder of the paper.

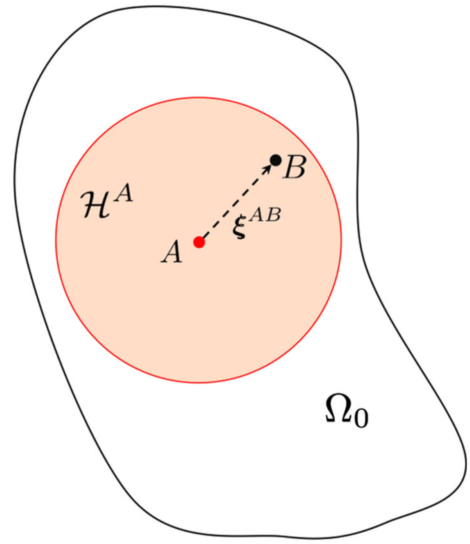

Fig. 2 Long-range interactions within the horizon of a given particle in the reference domain

For a hyperlastic material, the force state of particle A is a vector-valued function in $\mathbb{R}^d$ that is defined as

$$\underline{\boldsymbol{T}}^{AB}[\boldsymbol{x}^A, t]\langle\boldsymbol{\xi}^{AB}\rangle := \nabla_{\underline{\boldsymbol{Y}}^{AB}}\big[W(\underline{\boldsymbol{Y}}^{AB})\big], \quad \forall \mathbf{X}^B \in \mathcal{H}^A \tag{2}$$

where $W(\underline{\boldsymbol{Y}}^{AB})$ is the *strain energy density* per unit volume, which is selected to represent the constitutive properties of a given material. The force state is the conjugate measure of the deformation state, both of which are defined in the current configuration of the deformed body. The force state represented in Eq. (2) is the force per unit volume squared that particle A imposes onto particle B.

By definition, the force state that is imposed on particle A by B operates on bond $\boldsymbol{\xi}^{BA}$ and is defined $\underline{\boldsymbol{T}}^{BA}[\boldsymbol{x}^B, t]\langle\boldsymbol{\xi}^{BA}\rangle$ (see Fig. 3). One can assert that

$$\underline{\boldsymbol{T}}^{BA}[\boldsymbol{x}^B, t]\langle\boldsymbol{\xi}^{BA}\rangle = -\underline{\boldsymbol{T}}^{BA}[\boldsymbol{x}^B, t]\langle\boldsymbol{\xi}^{AB}\rangle \tag{3}$$

due to the property that each undeformed and deformed bond can be reversed. It is noted that the above assumption only holds for a specific class of elastic materials, namely ones that are of the following form

$$\begin{aligned} &\underline{\boldsymbol{T}}^{AB}[\boldsymbol{x}^A, t]\langle\boldsymbol{\xi}^{AB}\rangle = \boldsymbol{C}\boldsymbol{\xi}^{AB}, \quad \boldsymbol{C} \in \mathbb{R}^{d\times d} \\ &\underline{\boldsymbol{T}}^{AB}[\boldsymbol{x}^A, t]\langle\underline{\boldsymbol{Y}}^{AB}\rangle = \hat{\boldsymbol{C}}\underline{\boldsymbol{Y}}^{AB}, \quad \hat{\boldsymbol{C}} \in \mathbb{R}^{d\times d} \end{aligned} \tag{4}$$

where $\boldsymbol{C}$ and $\hat{\boldsymbol{C}}$ are second order tensors with respect to the action vectors $\boldsymbol{\xi}^{AB}$ and $\underline{\boldsymbol{Y}}^{\boldsymbol{AB}}$, respectively. This type of material response is typical for uses in non-ordinary state-based peridynamics, and it is assumed as the standard model for the remainder of this paper. Readers are referred to Silling and Lehoucq [29] and [26] for discussions of other force state definitions, such as those of bond-based materials.

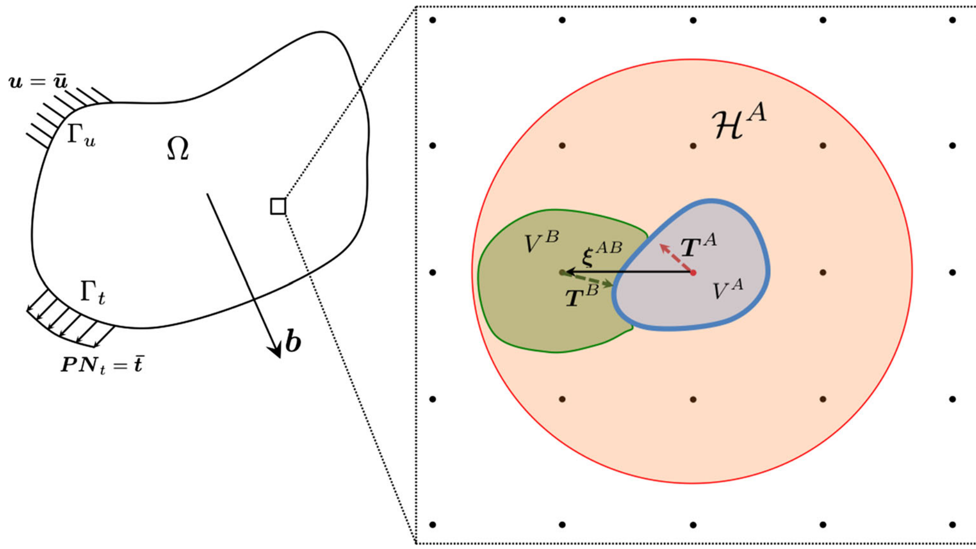

Fig. 3 Schematic illustration of the force state

Denoting $\rho_0(\boldsymbol{X}^A)$ as the density in the referential configuration and $\boldsymbol{B}(\boldsymbol{X}^A, t)$ as the body force per reference volume, the balance of energy in the context of the state-based peridynamics is expressed by using a Lagrangian potential of the following form,

$$
\begin{aligned}
L\big[\boldsymbol{u}(\boldsymbol{x}^A,t),\dot{\boldsymbol{u}}(\boldsymbol{x}^A,t)\big] = \int_{\Omega_0}\Big[\frac{1}{2}\rho_0(\boldsymbol{X}^A)\,\dot{\boldsymbol{u}}(\boldsymbol{x}^A,t)\cdot\dot{\boldsymbol{u}}(\boldsymbol{x}^A,t) \\
-\int_{\mathcal{H}^A}\Big(W(\underline{\boldsymbol{Y}}^{AB}) + W(\underline{\boldsymbol{Y}}^{BA})\Big)\,dV^B \\
+\boldsymbol{B}(\boldsymbol{X}^A,t)\cdot\boldsymbol{u}(\boldsymbol{x}^A,t)\Big]\,dV^A. \qquad (5)
\end{aligned}
$$

The integral term over the horizon of the particle A is the total strain energy density of all the bonds within $\mathcal{H}^A$. The velocity and displacement of particle A, $\boldsymbol{u}$ and $\dot{\boldsymbol{u}}$ respectively, are defined as

$$
\begin{cases}
\boldsymbol{u}(\boldsymbol{x}^A,t) := \boldsymbol{x}^A - \boldsymbol{X}^A = \boldsymbol{u}(\boldsymbol{x}^B,t) + \boldsymbol{\xi}^{AB} - \underline{\boldsymbol{Y}}^{AB}\langle\boldsymbol{\xi}^{AB}\rangle \\
\dot{\boldsymbol{u}}(\boldsymbol{x}^A,t) := \dot{\boldsymbol{x}}^A = \dot{\boldsymbol{u}}(\boldsymbol{x}^B,t) - \dot{\underline{\boldsymbol{Y}}}^{AB}\langle\boldsymbol{\xi}^{AB}\rangle
\end{cases}, \qquad (6)
$$

The potential function shown in Eq. (5) can be used to form an action functional,

$$
\mathcal{S}[\mathbf{u}(\mathbf{x}^A] := \int_{t_1}^{t_2} L\big[\boldsymbol{u}(\boldsymbol{x}^A,t),\dot{\boldsymbol{u}}(\boldsymbol{x}^A,t)\big]dt, \qquad (7)
$$

whose stationary condition is called the Hamiltonian principle, which yields the following Euler-Lagrange equations,

$$
\begin{aligned}
&\frac{d}{dt}\frac{\partial L}{\partial\dot{\boldsymbol{u}}(\boldsymbol{x}^A,t)} - \frac{\partial L}{\partial\boldsymbol{u}(\boldsymbol{x}^A,t)} \\
&= \int_{\Omega_0^A}\Big[\rho_0(\boldsymbol{X}^A)\,\ddot{\boldsymbol{u}}(\boldsymbol{x}^A,t) + \nabla_{\boldsymbol{u}(\boldsymbol{x}^A,t)}\int_{\mathcal{H}^A}\Big(\big[W(\underline{\boldsymbol{Y}}^{AB})\big] \\
&\quad+\big[W(\underline{\boldsymbol{Y}}^{BA})\big]\Big)\,dV^B - \boldsymbol{B}(\boldsymbol{X}^A,t)\Big]\,dV^B \\
&= \int_{\Omega_0^A}\Big[\rho_0(\boldsymbol{X}^A)\,\ddot{\boldsymbol{u}}(\boldsymbol{x}^A,t) - \int_{\mathcal{H}^A}\Big(\nabla_{\underline{\boldsymbol{Y}}^{AB}}\big[W(\underline{\boldsymbol{Y}}^{AB})\big] \\
&\quad-\nabla_{\underline{\boldsymbol{Y}}^{BA}}\big[W(\underline{\boldsymbol{Y}}^{BA})\big]\Big)\,dV^B - \boldsymbol{B}(\boldsymbol{X}^A,t)\Big]\,dV^B \\
&= \int_{\Omega_0^A}\Big[\rho_0(\boldsymbol{X}^A)\,\ddot{\boldsymbol{u}}(\boldsymbol{x}^A,t) - \int_{\mathcal{H}^A}\Big(\underline{\boldsymbol{T}}^{AB}\langle\boldsymbol{\xi}^{AB}\rangle \\
&\quad-\underline{\boldsymbol{T}}^{BA}\langle\boldsymbol{\xi}^{BA}\rangle\Big)\,dV^B - \boldsymbol{B}(\boldsymbol{X}^A,t)\Big]\,dV^B = \mathbf{0}, \qquad (8)
\end{aligned}
$$

where the chain rule and the reversibility of the bonds as stated in Eq. (3) are used to obtain the second integral formula in Eq. (8). The principle of the least action therefore corresponds to solving the following integro-differential equation,

$$
\begin{aligned}
&\int_{\mathcal{H}^A}\big[\underline{\boldsymbol{T}}^{AB}\langle\boldsymbol{\xi}^{AB}\rangle - \underline{\boldsymbol{T}}^{BA}\langle\boldsymbol{\xi}^{BA}\rangle\big]\,dV^B + \boldsymbol{B}(\boldsymbol{X}^A,t) \\
&= \rho_0(\boldsymbol{X}^A)\,\ddot{\boldsymbol{u}}(\boldsymbol{x}^A,t), \quad \forall\ \mathbf{X}^B \in \mathcal{H}^A, \quad \mathbf{X}^A \in \Omega_0 \qquad (9)
\end{aligned}
$$

which is defined as the peridynamics *equation of motion*. The integral of the force states over $\mathcal{H}^A$ is the peridynamics equivalent of the stress divergence used in classical continuum mechanics. In fact the expression of Eq. (9) closely resembles that of classical continuum mechanics, i.e.

$$
\nabla_{\mathbf{X}}\cdot\mathbf{P}(X,t) + \mathbf{B}(X,t) = \rho_0(X)\ddot{\mathbf{u}}(x,t).
$$

As was discussed in [7], the specific form of the peridynamic divergence operator corresponds to the mathematical notion of a nonlocal derivative that can be used to define nonlocal boundary-value problems.

$$\lim_{\delta^A \to 0} \left[\int_{\mathcal{H}^A} \left[\underline{\boldsymbol{T}}^{AB} \langle \boldsymbol{\xi}^{AB} \rangle - \underline{\boldsymbol{T}}^{BA} \langle \boldsymbol{\xi}^{BA} \rangle \right] dV^B \right] = \left[\nabla_{\mathbf{X}} \cdot \mathbf{P}(\boldsymbol{X}, t) \right] \Big|_{X = X^A}.$$

Thus it shows that the nonlocal peridynamics equation of motion converges to its localized counterpart in classical continuum mechanics as the horizon radius approaches zero.

3 Nonlocal differential operators

Non-ordinary state-based peridynamics was developed in [26], and it uses the concept of state variables to define measures that correlate to classical continuum mechanics. Common examples used in modeling Peridynamics elastic materials include the deformation gradient, and stress divergence. In this section, we illustrate that these two measures are intimately related through a nonlocal equivalent of a differential operator.

3.1 Total Lagrangian approach

In classical continuum mechanics, the total Lagrangian formulation describes field variables by their material derivative, which is defined as the derivatives with respect to the initial configuration of an undeformed body. Based on this approach, we propose the following nonlocal equivalent of a material gradient:

Definition 3.1 (*Nonlocal Material Differential Operators*) For any N-dimensional field function $G(\boldsymbol{X}) \in \mathbb{R}^{n_i \times \ldots n_N}$, $n_i \in \mathbb{Z}^+$ that satisfies the following properties:

1. Locally analytic at points A;
2. Integrable within the entire horizon $\mathcal{H}^A$, and
3. Exist a set of symmetric horizons that forms a cover for the physical domain Ω_0.

the nonlocal material gradient of $G(\boldsymbol{X})$ as a function of the average undeformed bonds $< \boldsymbol{\xi}^{AB} >$ at point A is defined as,

$$\mathcal{L}_X[G(\boldsymbol{X}^A)](< \boldsymbol{\xi}^{AB} >_X) := \left[\int_{\mathcal{H}^A} \omega(\xi^{AB})\, \Delta G^{AB}(\boldsymbol{X}) \otimes \boldsymbol{\xi}^{AB}\, dV^B \right] \mathbf{K}^{-1}, \qquad (10)$$

where $\xi^{AB} = \|\boldsymbol{\xi}^{AB}\|_2$, and the nonlocal material gradient of $G(\boldsymbol{X})$ as a function of the average deformed bonds $\underline{\boldsymbol{Y}}^{AB}$ at point A is defined as

$$\mathcal{L}_X\big[G(\boldsymbol{X}^A)\big]\big(< \mathbf{Y}^{AB} >_X \big) := \left[\int_{\mathcal{H}^A} \omega(\xi^{AB})\, \Delta G^{AB}(\boldsymbol{X}) \otimes \mathbf{Y}^{AB}\, dV^B \right] \mathbf{N}^{-T}, \qquad (11)$$

A nonlocal material divergence operator is constructed in a similar fashion as a function of the average undeformed bonds

$$\mathcal{M}_X\big[G(\boldsymbol{X}^A)\big]\big(< \boldsymbol{\xi}^{AB} >_X \big) := \int_{\mathcal{H}^A} \omega(\xi^{AB})\, \Delta G^{AB}(\boldsymbol{X}) \cdot \big(\mathbf{K}^{-1} \boldsymbol{\xi}^{AB}\big)\, dV^B \qquad (12)$$

and accordingly, as a function of the average deformed bonds

$$\mathcal{M}_X\big[G(\boldsymbol{X}^A)\big]\big(< \mathbf{Y}^{AB} >_X \big) := \int_{\mathcal{H}^A} \omega(\xi^{AB})\, \Delta G^{AB}(\boldsymbol{X}) \cdot \big(\mathbf{N}^{-1} \mathbf{Y}^{AB}\big)\, dV^B. \qquad (13)$$

In the above equations, $\Delta(\cdot)$ is defined as a *difference* operator in $\mathbb{R}^{n_i \times \ldots n_N}$, i.e.

$$\Delta G^{AB}(\mathbf{X}) := G(\mathbf{X}^B) - G(\mathbf{X}^A).$$

Here $\omega(\xi^{AB})$ is a window function (also referred to as the influence function) that is a scalar-valued positive function. It has two main purposes: first it helps to regularize the nonlocal integration, and second it imposes the following normalization condition,

$$\int_{\mathcal{H}^A} \omega(\xi^{AB}) dV^B = 1.$$

For simplicity, in this paper, the argument of the window function is chosen as $\xi^{AB} = \|\boldsymbol{\xi}^{AB}\|_2$, which is the length of the bond between particles A and B. Without further indication, it is assumed in this paper that the window function is carefully chosen so that no regularity issue will arise.

To explain the notation used in Eqs. (10)–(13), the arguments in these equations are defined as,

$$< \boldsymbol{\xi}^{AB} >_X := \int_{\mathcal{H}_A} \omega(\xi^{AB}) \boldsymbol{\xi}^{AB} dV^B, \quad \text{and}$$
$$< \mathbf{Y}^{AB} >_X := \int_{\mathcal{H}_A} \omega(\xi^{AB}) \mathbf{Y}^{AB} dV^B.$$

Besides reinforcing the the normalization condition, the window function can also be used as an agent to selectively modify bonds that are in voids, bonds between different materials, bonds that have exceeded their critical length, and numerous other scenarios including representation of uncertainty or statistical distribution of material strength. For simplicity, in this paper the window function is assumed to possess radial symmetry. Readers may consult [26] for more elaborate discussions on the window function in peridynamics, and [19] for a general explanation of the window functions in nonlocal continuum or particle methods.

Assume that $\mathcal{H}^A \subset \Omega_0 \subset \mathbb{R}^d$. $\boldsymbol{K}$ is commonly referred to as the shape tensor or moment tensor in $\mathcal{H}^A \times \mathcal{H}^A$ ([4,21]), and it is defined as,

$$\boldsymbol{K}(\boldsymbol{X}^A) := \int_{\mathcal{H}^A} \omega(\xi^{AB})\, \boldsymbol{\xi}^{AB} \otimes \boldsymbol{\xi}^{AB}\, dV^B. \tag{14}$$

The individual components of the shape tensor are a measure of the particle distribution inside the original horizon. As shown in [26], this tensor is symmetric and positive definite.

Assume that the deformed horizon $\mathcal{H}^A(t) \subset \Omega(t) \subset \mathbb{R}^d$. The $\boldsymbol{N}$ tensor is a two-point *shape* tensor in $\mathcal{H}^A(t) \times \mathcal{H}^A(0)$ (We use shorthanded notation $\mathcal{H}^A = \mathcal{H}^A(0)$ without causing confusion) with bases in both the reference and current configurations. It is formally defined as

$$\boldsymbol{N}\big(\boldsymbol{x}^A, \boldsymbol{X}^A\big) = \int_{\mathcal{H}^A} \omega(\xi^{AB})\, \boldsymbol{Y}^{AB}\langle \boldsymbol{\xi}^{AB}\rangle \otimes \boldsymbol{\xi}^{AB}\, dV^B. \tag{15}$$

In this paper, the above tensor is referred as the two-point tensor, because that $\boldsymbol{Y}^{AB} \in \Omega(t)$ and $\boldsymbol{\xi} \in \Omega_0$. This tensor is not necessarily symmetric nor positive definite because it depends on both the undeformed and deformed bond vectors. Note that at a given position A, both the shape tensor $\boldsymbol{K}$ and the $\boldsymbol{N}$ tensor are constants in the nonlocal differential operators shown in Eqs. (10)–(13) because they are definite integrations over the domain of the horizon.

Theorem 3.1 *The nonlocal gradient operators defined in Eqs.* (10) *and* (11) *converge to the localized gradient operator as the horizon radius approaches zero.*

$$\lim_{\delta^A \to 0} \mathcal{L}_X[G(\boldsymbol{X}^A)] = \big[\nabla_X G(\boldsymbol{X})\big]_{\boldsymbol{X}=\boldsymbol{X}^A}. \tag{16}$$

Proof We begin by proving the above limiting case for Eq. (10). Since $G(\boldsymbol{X})$ is analytic at the point A, it can be expressed through a convergent Taylor expansion as

$$\begin{aligned} G(\boldsymbol{X}) = G(\boldsymbol{X}^A) &+ \big[\nabla_X G(\boldsymbol{X}^A)\big]_{\boldsymbol{X}=\boldsymbol{X}^A} \cdot (\boldsymbol{X} - \boldsymbol{X}^A) \\ &+ \mathcal{O}\Big(\|\boldsymbol{X} - \boldsymbol{X}^A\|_2^2\Big) \end{aligned} \tag{17}$$

Substituting $\boldsymbol{X}$ with $\boldsymbol{X}^B \in \mathcal{H}^A$, we have

$$\begin{aligned} G(\boldsymbol{X}^B) - G(\boldsymbol{X}^A) &= \Delta^{AB} G(\boldsymbol{X}) \\ &= \big[\nabla_X G(\boldsymbol{X})\big]_{\boldsymbol{X}=\boldsymbol{X}^A} \cdot \boldsymbol{\xi}^{AB} + \mathcal{O}\Big(\|\boldsymbol{\xi}^{AB}\|_2^2\Big). \end{aligned} \tag{18}$$

We introduce the following notation for brevity

$$\boldsymbol{U} \circledast \boldsymbol{V} := \int_{\mathcal{H}^A} \omega(\xi^{AB})\, \boldsymbol{U} \otimes \boldsymbol{V}\, dV^B, \quad (\boldsymbol{U}, \boldsymbol{V}) \in \mathbb{R}^d,$$

and

$$\boldsymbol{U} \bullet \boldsymbol{V} := \int_{\mathcal{H}^A} \omega(\xi^{AB})\, \boldsymbol{U} \cdot \boldsymbol{V}\, dV^B, \quad (\boldsymbol{U}, \boldsymbol{V}) \in \mathbb{R}^d.$$

Inserting the finite difference operator $\Delta G(\boldsymbol{X})$ into the nonlocal differential operator of Eq. (10),

$$\begin{aligned} &\mathcal{L}_X\big[G(\boldsymbol{X}^A)\big](\langle \boldsymbol{\xi}^{AB}\rangle_X) \\ &= \Big[\Big(\big[\nabla_X G(\boldsymbol{X})\big]_{\boldsymbol{X}=\boldsymbol{X}^A} \cdot \boldsymbol{\xi}^{AB} + \mathcal{O}(\|\boldsymbol{\xi}^{AB}\|_2^2)\Big) \circledast \boldsymbol{\xi}^{AB}\Big]\mathbf{K}^{-1} \end{aligned} \tag{19}$$

Note that $G(\mathbf{X})$ is a tensorial fields in general, and the symbol $\mathcal{O}(\|\boldsymbol{\xi}^{AB}\|_2^2)$ should be understood as $\mathcal{O}(\|\boldsymbol{\xi}^{AB}\|_2^2)\mathbf{I}$, where unit tensor $\mathbf{I}$ has the dimension of $[\nabla_X G(\mathbf{X})]_{\mathbf{X}=\mathbf{X}^A} \cdot \boldsymbol{\xi}^{AB}$.

The nonlocal gradient has a second order remainder, which can be expanded in terms of the higher order terms. Thus, Eq. (19) may be further written as,

$$\begin{aligned} \mathcal{L}_X[G(\boldsymbol{X}^A)](\langle \boldsymbol{\xi}^{AB}\rangle_X) &= \big[\nabla_X G(\boldsymbol{X})\big]_{\boldsymbol{X}=\boldsymbol{X}^A} \cdot \boldsymbol{\xi}^{AB} \\ &+ \Big(\frac{1}{2}\nabla_X\big[\nabla_X G(\boldsymbol{X})\big]_{\boldsymbol{X}=\boldsymbol{X}^A} : (\boldsymbol{\xi}^{AB} \otimes \boldsymbol{\xi}^{AB})\Big) \circledast \boldsymbol{\xi}^{AB}\mathbf{K}^{-1} \\ &+ \Big(\frac{1}{6}\nabla_X\Big[\nabla_X\big[\nabla_X G(\boldsymbol{X})\big]\Big]_{\boldsymbol{X}=\boldsymbol{X}_\eta} \vdots (\boldsymbol{\xi}^{AB} \otimes \boldsymbol{\xi}^{AB} \otimes \boldsymbol{\xi}^{AB})\Big) \\ &\circledast \boldsymbol{\xi}^{AB}\mathbf{K}^{-1}, \end{aligned} \tag{20}$$

where $\mathbf{X}_\eta = \eta\mathbf{X}^A + (1-\eta)\mathbf{X}^B, \quad 0 \le \eta \le 1$. In above expression, the term consisting of $(\boldsymbol{\xi}^{AB} \otimes \boldsymbol{\xi}^{AB}) \circledast \boldsymbol{\xi}^{AB}$ is evaluated as an integral of an antisymmetric function over a symmetric domain, and hence it is zero. Therefore, the last term in Eq. (20) is the resulting truncation error. Noting that

$$\|(\boldsymbol{\xi}^{AB} \otimes \boldsymbol{\xi}^{AB} \otimes \boldsymbol{\xi}^{AB}) \circledast \boldsymbol{\xi}^{AB}\|_2 \sim \mathcal{O}(\|\boldsymbol{\xi}^{AB}\|_2^4) \quad \text{and} \quad \|\mathbf{K}\|_2 \sim \mathcal{O}(\|\boldsymbol{\xi}^{AB}\|_2^2),$$

the truncation error of (20) is of order $\mathcal{O}(\|\boldsymbol{\xi}^{AB}\|_2^2)$. This can be easily evaluated by considering a one-dimensional example with a constant window function $\tilde{\omega}$. Replacing $\boldsymbol{\xi}^{AB}$ with a one dimensional bond $X^\epsilon - X^A$, $X^A \equiv constant$, the truncation term becomes,

$$\begin{aligned} &\frac{1}{6}G'''(X_\eta)\int_{X^A-\delta^\epsilon}^{X^A+\delta^\epsilon} \tilde{\omega}(X^\epsilon - X^A)^4\, dX^\epsilon \\ &\times\Big[\int_{X^A-\delta^\epsilon}^{X^A+\delta^\epsilon} \tilde{\omega}(X^\epsilon - X^A)^2\, dX^\epsilon\Big]^{-1} = \frac{1}{10}G'''(X_\eta)(\delta^\epsilon)^2 \end{aligned} \tag{21}$$

where $X^A - \delta^\epsilon < X_\eta < X^A + \delta^\epsilon$, will converge to zero at a rate proportional to the square of the horizon size. Here it is assumed that the window function ω is chosen such that it ensures convergence of the above expression, as is discussed in [7]. It is also important to consider the practical implications for the above limit in the discrete case. Since it was assumed that the horizon is symmetric, this implies that as the horizon is refined, the particle density must remain the same for the entire horizon sequence.

Since the truncated terms (and thus the interpolation error) vanish in the limit as the horizon approaches zero, the limit in the above equation implies the validity of Eq. (16) when computing the nonlocal gradient by using Eq. (10).

The proof of the material gradient as a function of the deformed bonds follows the same procedure as above, simply replacing the differential operator with Eq. (11),

$$\begin{aligned}\mathcal{L}_X[G(\boldsymbol{X}^A)](<\boldsymbol{Y}^{AB}>_X) = \Bigg[&\Big[\nabla_X G(\boldsymbol{X})\Big]_{X=X^A}\cdot\boldsymbol{\xi}^{AB} \\ &+\Big(\frac{1}{2}\nabla_X\big[\nabla_X G(\boldsymbol{X})\big]_{X=X^A}:(\boldsymbol{\xi}^{AB}\otimes\boldsymbol{\xi}^{AB})\Big) \\ &+\Bigg[\frac{1}{6}\nabla_X\Big[\nabla_X\big[\nabla_X G(\boldsymbol{X})\big]\Big]_{X=X_\eta}\vdots(\boldsymbol{\xi}^{AB}\otimes\boldsymbol{\xi}^{AB}\otimes\boldsymbol{\xi}^{AB})\Big)\Bigg] \\ &\circledast\mathbf{Y}^{AB}\mathbf{N}^{-T},\end{aligned} \tag{22}$$

where $\mathbf{X}_\eta := \eta\mathbf{X}^A + (1-\eta)\mathbf{X}^B, \quad 0\le\eta\le 1.$

As will be discussed in the next Section, an approximation of the deformed bonds are obtained through a linear mapping of the undeformed bonds

$$\underline{\boldsymbol{Y}}^{AB} = \boldsymbol{\mathcal{F}}_A\boldsymbol{\xi}^{AB} + \mathcal{O}(\|\boldsymbol{\xi}^{AB}\|_2^2), \quad \boldsymbol{\mathcal{F}}_A \in \mathcal{H}^A(t)\times\mathcal{H}^A(0).$$

$\boldsymbol{\mathcal{F}}_A$ is constant within the horizon of A. With this assumption, the second term in the right-hand side of Eq. (22) will be zero, due to the antisymmetry of the integral. Therefore, the highest order remainder will be of order $\mathcal{O}(\|\boldsymbol{\xi}^{AB}\|_2^2)$.

As a side remark, the analyticity of the function $G(\boldsymbol{X})$ at points A and B requires the function to be infinitely differentiable and continuous at these points. This inherently means that all higher order derivatives, and thus the truncation error, are bounded. If the deformation field is not continuous and/or smooth at any specific point, the convergence may not necessarily obey the properties formulated above. Readers are referred to recent studies in Mengesha and Du [23] that examine convergence properties of nonlocal differential operators with minimal constraints on continuity. □

Using the same procedures done above, one can easily show that the nonlocal material divergence operator converges to its local counterpart. This leads to the following proposition.

Theorem 3.2 *The nonlocal divergence operators defined in Eqs. (12) and (13) converge to the localized divergence operator as the horizon radius approaches zero.*

$$\lim_{\delta^A\to 0}\mathcal{M}_X[G(\boldsymbol{X}^A)] = \big[\nabla_X\cdot G(\boldsymbol{X})\big]_{X=X^A} \tag{23}$$

Proof Inserting the exact differential in Eq. (18) into the nonlocal divergence operator that acts on the undeformed bonds in Eq. (12), we obtain the following expression,

$$\begin{aligned}&\mathcal{M}_X[G(\boldsymbol{X}^A)](<\boldsymbol{\xi}^{AB}>_X) \\ &=\Big[\Big(\big[\nabla_X G(\boldsymbol{X})\big]_{X=X^A}\cdot\boldsymbol{\xi}^{AB}+\mathcal{O}(\|\boldsymbol{\xi}^{AB}\|_2^2)\Big)\bullet\mathbf{K}^{-1}\boldsymbol{\xi}^{AB}\Big] \\ &=\big[\nabla_X G(\boldsymbol{X})\big]_{X=X^A}:\boldsymbol{I}+\Big(\mathcal{O}(\|\boldsymbol{\xi}^{AB}\|_2^2)\Big)\bullet\mathbf{K}^{-1}\boldsymbol{\xi}^{AB} \\ &=\big[\nabla_X\cdot G(\boldsymbol{X})\big]_{X=X^A}+\Big(\mathcal{O}(\|\boldsymbol{\xi}^{AB}\|_2^2)\Big)\bullet\mathbf{K}^{-1}\boldsymbol{\xi}^{AB}\end{aligned} \tag{24}$$

Similarly, inserting the exact differential into the divergence operator that acts on the deformed bonds

$$\begin{aligned}&\mathcal{M}_X[G(\boldsymbol{X}^A)](<\boldsymbol{Y}^{AB}>_X) \\ &=\Big[\Big(\big[\nabla_X G(\boldsymbol{X})\big]_{X=X^A}\cdot\boldsymbol{\xi}^{AB}+\mathcal{O}(\|\boldsymbol{\xi}^{AB}\|_2^2)\Big)\bullet\mathbf{N}^{-1}\underline{\boldsymbol{Y}}^{AB}\Big] \\ &=\big[\nabla_X G(\boldsymbol{X})\big]_{X=X^A}:\boldsymbol{I}+\Big(\mathcal{O}(\|\boldsymbol{\xi}^{AB}\|_2^2)\Big)\bullet\mathbf{N}^{-1}\underline{\boldsymbol{Y}}^{AB} \\ &=\big[\nabla_X\cdot G(\boldsymbol{X})\big]_{X=X^A}+\Big(\mathcal{O}(\|\boldsymbol{\xi}^{AB}\|_2^2)\Big)\bullet\mathbf{N}^{-1}\underline{\boldsymbol{Y}}^{AB}\end{aligned} \tag{25}$$

Following an identical procedure as was done for the gradient operators, the first remainder term is zero due to the antisymmetry of the integral for both nonlocal divergence operators in Eqs. (12) and (13), assuming continuity and smoothness for points A and B. The truncation error is therefore of order $\mathcal{O}(\|\boldsymbol{\xi}^{AB}\|_2^2)$, thus proving the above Proposition. □

The nonlocal differential operators can be viewed in a broader sense as weighted directional integral operators or nonlocal directional derivative. For instance, a generalized nonlocal gradient operator can have the following form

$$\begin{aligned}&\tilde{\mathcal{L}}_X[G(\boldsymbol{X}^A)](<\Delta\boldsymbol{w}>_X) \\ &=\Big[\int_{\mathcal{H}^A}\omega(\xi^{AB})\,\Delta G(\boldsymbol{X})\otimes\Delta\boldsymbol{w}\,dV^B\Big] \\ &\quad\times\Big[\int_{\mathcal{H}^A}\omega(\xi^{AB})\Delta\boldsymbol{w}\otimes\boldsymbol{\xi}^{AB}\,dV^B\Big]^{-T}, \\ &\text{where}\quad \Delta\boldsymbol{w}\in\mathbb{R}^d\end{aligned} \tag{26}$$

with the vector difference $\Delta\boldsymbol{w} := \boldsymbol{w}^B - \boldsymbol{w}^A$ denoting the directional vector; and the term,

$$\Delta\boldsymbol{w}\Big[\int_{\mathcal{H}^A}\omega(\xi^{AB})\quad\Delta\boldsymbol{w}\otimes\boldsymbol{\xi}^{AB}\quad dV^B\Big]^{-T},$$

defines a the weighted directional vector.

The above formulation also satisifies the convergence properties shown in this section. The selection of the weight function as the material positions will generate a differential of the undeformed bonds, and thus the above formula is equivalent to Eq. (10). Likewise, selecting the differential of the weight function as the deformed bonds, we obtain Eq. (11).

It is worthy noting that the relation between this general formulation and the weighted nonlocal adjoint operator obtained in [8] can be expressed as

$$\mathcal{D}^*_\omega(\boldsymbol{u})(\boldsymbol{X}) = \int_{\mathcal{H}^A} \omega(\xi^{AB})(\boldsymbol{u}^A - \boldsymbol{u}^B) \otimes \boldsymbol{\alpha}(\boldsymbol{X}^A, \boldsymbol{X}^B)\, dV^B \tag{27}$$

The general weight function $\boldsymbol{\alpha}$ used in [8] is defined as an anti-symmetric vector in $\mathbb{R}^d$. If it is defined as the negative contraction of the undeformed bond vector with the shape tensor $\boldsymbol{\alpha} = -\boldsymbol{\xi}\boldsymbol{K}^{-1}$, one obtains Eq. (10). Similarly, selecting the weight function as the negative contraction of the deformed bond $\underline{\boldsymbol{Y}}$ with the $\boldsymbol{N}$ tensor, Eq. (11) is obtained. Note that the gradient operator that acts on the deformed bonds does not obey the antisymmetry of the weight function $\boldsymbol{\alpha}$ that is assumed in the nonlocal differential operator shown above. Even with this key distinction, the differential operator in Eq. (11) retains an identical convergence rate to its antisymmetric counterpart in Eq. (10).

In fact, the nonlocal material differential operator can be understood as,

$$\begin{aligned}\nabla_X \otimes \Big(\bullet\Big) &\rightarrow \lim_{\Delta\mathbf{X}\to 0} \frac{1}{\Delta\mathbf{X}}\Big(\Delta(\bullet)\Big)\\ &:= \lim_{\delta^A\to 0}\left[\int_{\mathcal{H}^A} \omega(\xi^{AB})\Big(\Delta(\bullet)\Big)\otimes \boldsymbol{\xi}^{AB}\, dV\right]\mathbf{K}^{-1}\end{aligned} \tag{28}$$

where δ^A is the radius of $\mathcal{H}^A$. It should be noted that the above limit process is such that the particle density inside the horizon will remain the same as $\delta^A \to 0$.

Adopting this notation, we can also define a nonlocal material divergence operator as

$$\begin{aligned}\nabla\cdot\Big(\bullet\Big) &\rightarrow \lim_{\Delta\mathbf{X}\to 0} \mathrm{Tr}\Big(\frac{1}{\Delta\mathbf{X}}\Big(\Delta(\bullet)\Big)\Big)\\ &:= \lim_{\delta^A\to 0}\left[\int_{\mathcal{H}^A} \omega(\xi^{AB})\Big(\Delta(\bullet)\Big)\cdot \boldsymbol{\xi}^{AB}\, dV^B\right]\mathbf{K}^{-1}\end{aligned} \tag{29}$$

Since $\mathbf{K}^{-1}$ is symmetric, Eq. (29) may be rewritten as

$$\int_{\mathcal{H}^A} \omega(\xi^{AB})\Big(\Delta(\bullet)\Big)\cdot(\mathbf{K}^{-1}\boldsymbol{\xi}^{AB})\, dV^B \tag{30}$$

This formulation of the gradient and divergence operators has been briefly discussed in Ren et al. [24].

3.1.1 Deformation gradient

Traditional continuum mechanics incorporates a two-point tensor called the *deformation gradient* as a means of mapping localized differential tangent vectors from the reference (material) configuration to the current (spatial) configuration. Non-ordinary state-based peridynamics utilizes a similar approach whereby a "deformation gradient" $\boldsymbol{F}$ is introduced as a mapping mechanism based on the deformed horizon as

$$\underline{\boldsymbol{Y}}^{AB}\langle\boldsymbol{\xi}^{AB}\rangle = \boldsymbol{\mathcal{F}}_A\big(\boldsymbol{x}^A, \boldsymbol{X}^A\big)\cdot\boldsymbol{\xi}^{AB} + \mathcal{O}\Big(\|\boldsymbol{\xi}^{AB}\|_2^2\Big), \tag{31}$$

where the subscript in $\boldsymbol{\mathcal{F}}_A$ indicates the dependency on the collection of deformed and undeformed bonds in the horizon of particle A. As in classical continuum mechanics, the deformation gradient in peridynamics is a second-order two-point tensor in $\Omega(t) \times \Omega_0$. Furthermore, in the context of nano-mechanics or physics, the homogeneous deformation that satisfies Eq. (31) is referred as the local deformation that obeys the *the Cauchy-Born rule* e.g. [9,32].

Proposition 3.3 *Given a point $\mathbf{X}^A \in \Omega_0$ with neighbors $\mathbf{X}^B \in \mathcal{H}^A$ that undergo a deformation field that satisfies the requirements of the nonlocal gradient operators, a deformation gradient is constructed as a function of the undeformed bonds as*

$$\boldsymbol{F}_A := \mathbf{F}\big(\boldsymbol{x}^A, \boldsymbol{X}^A\big)\langle\boldsymbol{\xi}^{AB}\rangle = \boldsymbol{N}\big(\boldsymbol{x}^A, \boldsymbol{X}^A\big)\cdot\boldsymbol{K}^{-1}(\boldsymbol{X}^A), \tag{32}$$

or, alternatively, as a function of the deformed bonds as

$$\hat{\mathbf{F}}_A := \hat{\mathbf{F}}\langle\boldsymbol{Y}^{AB}\rangle = \boldsymbol{M}\big(\boldsymbol{x}^A\big)\cdot\boldsymbol{N}^{-T}\big(\boldsymbol{x}^A, \boldsymbol{X}^A\big). \tag{33}$$

Proof The peridynamic deformation gradient is essentially a nonlocal gradient of the current position of particle A with respect to its reference position. It can therefore be derived utilizing the nonlocal material gradient in Eq. (10) with the nonlocal differential of the current position

$$\begin{aligned}\mathbf{F}_A &= \boldsymbol{F}\big(\boldsymbol{x}^A, \boldsymbol{X}^A\big)\langle\boldsymbol{\xi}^{AB}\rangle\\ &= \left[\int_{\mathcal{H}^A}\omega(\xi^{AB})\Delta\boldsymbol{x}\otimes\boldsymbol{\xi}^{AB}\, dV^B\right]\boldsymbol{K}^{-1}(\boldsymbol{X}^A)\\ &= \left[\int_{\mathcal{H}^A}\omega(\xi^{AB})\underline{\boldsymbol{Y}}^{AB}\otimes\boldsymbol{\xi}^{AB}\, dV^B\right]\boldsymbol{K}^{-1}(\boldsymbol{X}^A)\\ &= \boldsymbol{N}\big(\boldsymbol{x}^A, \boldsymbol{X}^A\big)\cdot\boldsymbol{K}^{-1}(\boldsymbol{X}^A)\end{aligned} \tag{34}$$

An alternative deformation gradient can also be constructed as a mapping function of the deformed bonds

$$\begin{aligned}\hat{\mathbf{F}}_A &= \boldsymbol{F}\big(\boldsymbol{x}^A, \boldsymbol{X}^A\big)\langle \boldsymbol{Y}^{AB}\rangle \\ &= \Big[\int_{\mathcal{H}^A} \omega(\xi^{AB})\Delta \boldsymbol{x} \otimes \underline{\boldsymbol{Y}}^{AB}\, dV^B\Big]\boldsymbol{N}^{-T}\big(\boldsymbol{x}^A, \boldsymbol{X}^A\big) \\ &= \Big[\int_{\mathcal{H}^A} \omega(\xi^{AB})\underline{\boldsymbol{Y}}^{AB} \otimes \underline{\boldsymbol{Y}}^{AB}\, dV^B\Big]\boldsymbol{N}^{-T}\big(\boldsymbol{x}^A, \boldsymbol{X}^A\big) \\ &= \boldsymbol{M}\big(\boldsymbol{x}^A\big) \cdot \boldsymbol{N}^{-T}\big(\boldsymbol{x}^A, \boldsymbol{X}^A\big) \end{aligned} \tag{35}$$

where $\boldsymbol{M}$ is the deformed shape tensor that is defined as

$$\begin{aligned}\boldsymbol{M}\big(\boldsymbol{x}^A\big) &:= \int_{H^A(t)} \omega_t(Y^{AB})\underline{\boldsymbol{Y}}^{AB} \otimes \underline{\boldsymbol{Y}}^{AB} \\ dv^B &:= \int_{H^A} \omega(\xi^{AB})\underline{\boldsymbol{Y}}^{AB} \otimes \underline{\boldsymbol{Y}}^{AB} dV^B \end{aligned} \tag{36}$$

where $Y^{AB} := \|\mathbf{Y}^{AB}\|_2$, and $\boldsymbol{M}$ describes a measure of the shape of the particle distribution inside the horizon in the current configuration $\Omega(t)$. □

We note in passing that in general $\omega_t(Y^{AB}) \neq \omega(\xi^{AB})$. We post a condition on the window function,

$$\omega_t(Y^{AB})dv^B = \omega(\xi^{AB})dV^B \quad \rightarrow \quad \omega_t(V^{AB}) = J^{-1}\omega(\xi^{AB}),$$

so that the window function is understood as an equivalent density distribution function, i.e. $\rho_t \sim \omega_t(Y^{AB})$ and $\rho_0 \sim \omega(\xi^{AB})$. Various fundamental properties that hold for the shape tensor of the undeformed configuration $\boldsymbol{K}$ also hold for $\boldsymbol{M}$.

Lemma 3.4 *The deformed shape tensor $\boldsymbol{M}$ is symmetric, thus obeying the transpose property,*

$$\boldsymbol{M} = \boldsymbol{M}^T.$$

Proof The proof is fairly trivial. The transpose of the deformed shape tensor is performed by switching the first and second entries of the outer product

$$\begin{aligned}\boldsymbol{M}^T &= \Big[\int_{\mathcal{H}^A(t)} \omega_t(Y^{AB})\underline{\boldsymbol{Y}}^{AB} \otimes \underline{\boldsymbol{Y}}^{AB}\, dv^B\Big]^T \\ &= \int_{\mathcal{H}^A(t)} \omega_t(Y^{AB})\underline{\boldsymbol{Y}}^{AB} \otimes \underline{\boldsymbol{Y}}^{AB}\, dv^B \\ &= \boldsymbol{M}. \end{aligned} \tag{37}$$

□

The deformed shape tensor is also diagonalizable, with real eigenvalues $\lambda_i, i = 1, \ldots, d$ and eigenvectors $\boldsymbol{v}_i$. The eigenvalues are also positive because they represent the deformed bonds squared in the configuration of the eigenvectors. Therefore, one can easily show that $\boldsymbol{M}$ is positive definite by utilizing the spectral decomposition theorem

$$\boldsymbol{w} \cdot \boldsymbol{M}\boldsymbol{w} = \boldsymbol{w} \cdot \Big[\sum_{i=1}^{d} \lambda_i\, \boldsymbol{v}_i \otimes \boldsymbol{v}_i\Big]\boldsymbol{w} \geq 0, \quad \forall \boldsymbol{w} \in \mathbb{R}^d. \tag{38}$$

In contrast with the standard deformation gradient in classical continuum mechanics, the peridynamics deformation gradient is a nonlocal measure, because it takes into account bonds at finite distances within a given horizon. The nonlocal gradient operator as defined in the previous sections only assumes local analyticity at points A and B. In the discrete setting, there is no restriction on the continuity requirements on the horizon domain that excludes points A and B, $\mathcal{H}^A \backslash \{\boldsymbol{X}^A, \boldsymbol{X}^B\}$. As a direct result, the deformation gradient as expressed above can be non-singular in the presence of strong discontinuities within $\mathcal{H}^A \backslash \{\boldsymbol{X}^A, \boldsymbol{X}^B\}$.

The limit in Eq. (16) implies that as the horizon radius approaches zero, the value of the nonlocal deformation gradient approaches the local one. In other words, as the radius of the horizon decreases, the accuracy of the deformation gradient increases, and the approximated deformed bond vectors $\underline{\boldsymbol{Y}}'$ that are mapped by the deformation gradient of Eqs. (32) and (33) will approach the actual values of the deformed bond vectors $\underline{\boldsymbol{Y}}$, as illustrated in Fig. 4. One can also reduce the approximation errors by formulating a deformation gradient based on higher order nonlocal differential operators. As was shown in Li et al. [18], higher order approximations will, in general, reduce the error. However, they will also require higher computational effort and costs.

As a side remark, according to Eq. (16), the both deformation gradients that act on the undeformed and deformed bonds will converge at the same rate, because their truncation errors are equivalent in order.

Proposition 3.5 *Given an affine deformation field, such as a uniform stretch and/or a rigid translation $\boldsymbol{C}(t)$*

$$\underline{\boldsymbol{Y}}^{AB}(t) = \boldsymbol{\mathcal{F}}_A(t) \cdot \boldsymbol{\xi}^{AB} + \boldsymbol{C}(t), \quad \forall \mathbf{X}^B \in \mathcal{H}^A \tag{39}$$

The nonlocal deformation gradient is equivalent to its localized counterpart $\boldsymbol{\mathcal{F}}^{AB}$ in classical continuum mechanics.

Proof In this case, the exact deformation gradient acts as a linear operator. If we use the deformation gradient that acts on the undeformed bond,

$$\begin{aligned}\mathbf{F}_A =& \Big[\int_{\mathcal{H}^A} \omega(\xi^{AB})\, \underline{\boldsymbol{Y}}^{AB} \otimes \boldsymbol{\xi}^{AB}\, dV^B\Big] \\ &\times \Big[\int_{\mathcal{H}^A} \omega(\xi^{AB})\, \boldsymbol{\xi}^{AB} \otimes \boldsymbol{\xi}^{AB}\, dV^B\Big]^{-1}\end{aligned}$$

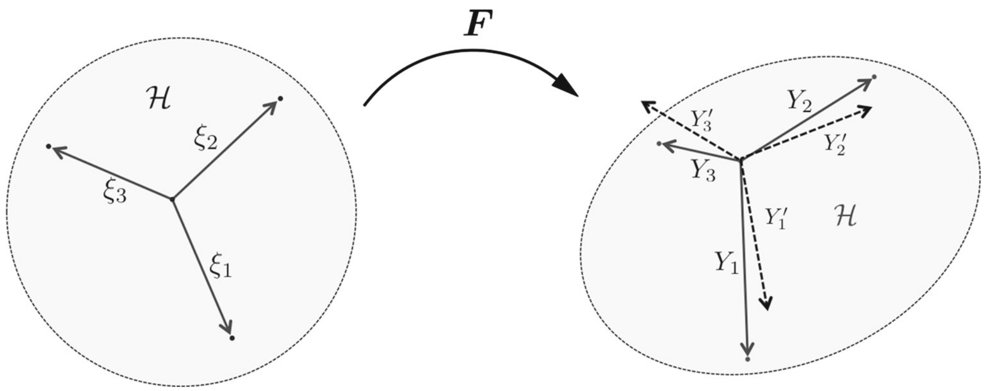

Fig. 4 The Mapping mechanism of the peridynamics deformation gradient

$$
\begin{aligned}
&= \left[\int_{\mathcal{H}^A} \omega(\xi^{AB})\,(\boldsymbol{\mathcal{F}}_A\cdot\boldsymbol{\xi}^{AB})\otimes\boldsymbol{\xi}^{AB}\,dV^B\right] \\
&\quad\times\left[\int_{\mathcal{H}^A} \omega(\xi^{AB})\,\boldsymbol{\xi}^{AB}\otimes\boldsymbol{\xi}^{AB}\,dV^B\right]^{-1} \\
&= \boldsymbol{\mathcal{F}}_A\cdot\left[\int_{\mathcal{H}^A} \omega(\xi^{AB})\,\boldsymbol{\xi}^{AB}\otimes\boldsymbol{\xi}^{AB}\,dV^B\right] \\
&\quad\times\left[\int_{\mathcal{H}^A} \omega(\xi^{AB})\,\boldsymbol{\xi}^{AB}\otimes\boldsymbol{\xi}^{AB}\,dV^B\right]^{-1} \\
&= \boldsymbol{\mathcal{F}}_A.
\end{aligned} \tag{40}
$$

This proof coincides with what was presented in [26]. As an extension, one can show that the deformation gradient that acts on the deformed bonds also satisfies the above proposition,

$$
\begin{aligned}
\hat{\mathbf{F}}_A &= \left[\int_{\mathcal{H}^A(t)} \omega_t(Y^{AB})\,\underline{\boldsymbol{Y}}^{AB}\otimes\underline{\boldsymbol{Y}}^{AB}\,dv^B\right] \\
&\quad\times\left[\int_{\mathcal{H}^A} \omega(\xi^{AB})\,\boldsymbol{\xi}^{AB}\otimes\underline{\boldsymbol{Y}}^{AB}\,dV^B\right]^{-1} \\
&= \left[\int_{\mathcal{H}^A} \omega(\xi^{AB})\,(\boldsymbol{\mathcal{F}}_A\cdot\boldsymbol{\xi}^{AB})\otimes(\boldsymbol{\mathcal{F}}_A\cdot\boldsymbol{\xi}^{AB})\,dV^B\right] \\
&\quad\times\left[\int_{\mathcal{H}^A} \omega(\xi^{AB})\,\boldsymbol{\xi}^{AB}\otimes(\boldsymbol{\mathcal{F}}^{AB}\cdot\boldsymbol{\xi}^{AB})\,dV^B\right]^{-1} \\
&= \boldsymbol{\mathcal{F}}_A\cdot\left[\int_{\mathcal{H}^A} \omega(\xi^{AB})\,\boldsymbol{\xi}^{AB}\otimes\boldsymbol{\xi}^{AB}\,dV^B\right] \\
&\quad\cdot\left((\boldsymbol{\mathcal{F}}_A)^T(\boldsymbol{\mathcal{F}}_A)^{-T}\right) \\
&\quad\times\left[\int_{\mathcal{H}^A} \omega(\xi^{AB})\,\boldsymbol{\xi}^{AB}\otimes\boldsymbol{\xi}^{AB}\,dV^B\right]^{-1} \\
&= \boldsymbol{\mathcal{F}}_A.
\end{aligned} \tag{41}
$$

□

3.1.2 Nonlocal material stress divergence

The force state introduced into the equation of motion in Sect. 2 acts as a vector quantity that when integrated within the horizon of a given particle, which represents an approximation to the divergence of the stress field in the current configuration basis.

Proposition 3.6 *Given a point $\mathbf{X}^A \in \Omega_0$ and neighbors $\mathbf{X}^B \in \mathcal{H}^A$ that contain a non-zero stress and satisfy the conditions of Definition (3.1), the nonlocal material divergence of the first Piola-Kirchhoff stress tensor is expressed as a function of the deformed bonds as*

$$
\begin{aligned}
&\mathcal{M}_X[\boldsymbol{P}(\boldsymbol{x}^A,t)](<\boldsymbol{\xi}^{AB}>_X) \\
&\quad= -\int_{\mathcal{H}^A} \omega(\xi^{AB})\left(\underline{\boldsymbol{T}}^{BA}\langle\boldsymbol{\xi}^{BA}\rangle+\underline{\boldsymbol{T}}^{AB}\langle\boldsymbol{\xi}^{AB}\rangle\right)dV^B,
\end{aligned} \tag{42}
$$

where the force state $\underline{\boldsymbol{T}}\langle\boldsymbol{\xi}\rangle$ is defined as

$$
\begin{aligned}
\underline{\boldsymbol{T}}^{AB}[\boldsymbol{x}^A,t]\langle\boldsymbol{\xi}^{AB}\rangle &:= \boldsymbol{P}\left(\boldsymbol{x}^A,t\right)\cdot\boldsymbol{K}^{-1}(\boldsymbol{X}^A)\boldsymbol{\xi}^{AB} \\
\underline{\boldsymbol{T}}^{BA}[\boldsymbol{x}^B,t]\langle\boldsymbol{\xi}^{BA}\rangle &:= \boldsymbol{P}\left(\boldsymbol{x}^B,t\right)\cdot\boldsymbol{K}^{-1}(\boldsymbol{X}^A)\boldsymbol{\xi}^{BA}
\end{aligned} \tag{43}
$$

The material stress divergence as a function of the deformed bonds is expressed as

$$
\begin{aligned}
&\mathcal{M}_X[\boldsymbol{P}(\boldsymbol{x}^A,t)](<\boldsymbol{Y}^{AB}>_X) \\
&\quad= -\int_{\mathcal{H}^A} \omega(\xi^{AB})\left(\underline{\boldsymbol{T}}^{BA}\langle\underline{\boldsymbol{Y}}^{BA}\rangle+\underline{\boldsymbol{T}}^{AB}\langle\underline{\boldsymbol{Y}}^{AB}\rangle\right)dV^B
\end{aligned} \tag{44}
$$

where the force state $\underline{\boldsymbol{T}}\langle\underline{\boldsymbol{Y}}\rangle$ is defined as

$$
\begin{aligned}
\underline{\boldsymbol{T}}^{AB}[\boldsymbol{x}^A,t]\langle\underline{\boldsymbol{Y}}^{AB}\rangle &:= \boldsymbol{P}\left(\boldsymbol{x}^A,t\right)\cdot\boldsymbol{N}^{-1}(\boldsymbol{x}^A,\boldsymbol{X}^A)\underline{\boldsymbol{Y}}^{AB} \\
\underline{\boldsymbol{T}}^{BA}[\boldsymbol{x}^B,t]\langle\underline{\boldsymbol{Y}}^{BA}\rangle &:= \boldsymbol{P}\left(\boldsymbol{x}^B,t\right)\cdot\boldsymbol{N}^{-1}(\boldsymbol{x}^A,\boldsymbol{X}^A)\underline{\boldsymbol{Y}}^{BA}.
\end{aligned} \tag{45}
$$

Proof To formulate a nonlocal analog of the material divergence of the first Piola-Kirchhoff stress tensor $\boldsymbol{P}$ as a function of the undeformed bonds, Eq. (10) can be applied to a differential in the stresses for a given particle A and its neighbors $\mathbf{X}^B \in \mathcal{H}^A$

$$\begin{aligned}
&\mathcal{M}_X[\boldsymbol{P}(\boldsymbol{x}^A,t)](<\boldsymbol{\xi}^{AB}>_X)\\
&=\int_{\mathcal{H}^A}\omega(\xi^{AB})\,\Delta\boldsymbol{P}(\boldsymbol{x},t)\cdot\left(\mathbf{K}^{-1}(\boldsymbol{X}^A)\boldsymbol{\xi}^{AB}\right)dV^B\\
&=\int_{\mathcal{H}^A}\omega(\xi^{AB})\left(\boldsymbol{P}(\boldsymbol{x}^B,t)-\boldsymbol{P}(\boldsymbol{x}^A,t)\right)\\
&\quad\cdot\left(\mathbf{K}^{-1}(\boldsymbol{X}^A)\boldsymbol{\xi}^{AB}\right)dV^B\\
&=-\int_{\mathcal{H}^A}\omega(\xi^{AB})\left(\underline{\boldsymbol{T}}^{BA}\langle\boldsymbol{\xi}^{BA}\rangle+\underline{\boldsymbol{T}}^{AB}\langle\boldsymbol{\xi}^{AB}\rangle\right)dV^B.
\end{aligned}\tag{46}$$

The proof of the nonlocal stress divergence of the first Piola-Kirchhoff stress tensor in terms of the deformed bonds follows an identical procedure as above, simply by utilizing the differential operator in Eq. (11),

$$\begin{aligned}
&\mathcal{M}_X[\boldsymbol{P}(\boldsymbol{x}^A,t)](<\boldsymbol{Y}^{AB}>_X)\\
&=\int_{\mathcal{H}^A}\omega(\xi^{AB})\,\Delta\boldsymbol{P}(\boldsymbol{x},t)\cdot\left(\mathbf{N}^{-1}(\boldsymbol{x}^A,\boldsymbol{X}^A)\underline{\boldsymbol{Y}}^{AB}\right)dV^B\\
&=\int_{\mathcal{H}^A}\omega(\xi^{AB})\left(\boldsymbol{P}(\boldsymbol{x}^B,t)-\boldsymbol{P}(\boldsymbol{x}^A,t)\right)\\
&\quad\cdot\left(\mathbf{N}^{-1}(\boldsymbol{x}^A,\boldsymbol{X}^A)\underline{\boldsymbol{Y}}^{AB}\right)dV^B\\
&=-\int_{\mathcal{H}^A}\omega(\xi^{AB})\left(\underline{\boldsymbol{T}}^{BA}\langle\underline{\boldsymbol{Y}}^{BA}\rangle+\underline{\boldsymbol{T}}^{AB}\langle\underline{\boldsymbol{Y}}^{AB}\rangle\right)dV^B.
\end{aligned}\tag{47}$$

□

Proposition 3.7 *Given that balance of linear momentum is locally satisfied for each point A in the reference domain* Ω_0

$$\int_{\Omega_0}\left[\nabla_X\cdot\boldsymbol{P}(\boldsymbol{x}^A,t)+\boldsymbol{B}(\boldsymbol{X}^A,t)\right]dV=\int_{\Omega_0}\rho_0(\boldsymbol{X}^A)\ddot{\boldsymbol{u}}(\boldsymbol{X}^A,t)\,dV,\quad\forall\mathbf{X}^A\in\Omega_0\tag{48}$$

the nonlocal balance of linear momentum will also be satisfied in the limit as the horizon radius approaches zero, thus yielding the equation of motion for each point A given as a function of the undeformed bonds as

$$-\int_{\mathcal{H}^A}\omega(\xi^{AB})\underline{\boldsymbol{T}}^{BA}\langle\boldsymbol{\xi}^{BA}\rangle\,dV^B+\boldsymbol{B}(\boldsymbol{X}^A,t)=\rho_0(\boldsymbol{X}^A,t)\ddot{\boldsymbol{u}}^A(\boldsymbol{x}^A,t),\quad\forall\mathbf{X}^A\in\Omega_0,\quad\mathbf{X}^B\in\mathcal{H}^A\tag{49}$$

and as a function of the deformed bonds as

$$\begin{aligned}
&-\int_{\mathcal{H}^A}\omega(\xi^{AB})\big(\underline{\boldsymbol{T}}^{AB}\langle\underline{\boldsymbol{Y}}^{AB}\rangle\\
&\quad+\underline{\boldsymbol{T}}^{BA}\langle\underline{\boldsymbol{Y}}^{BA}\rangle\big)\,dV^B+\boldsymbol{B}(\boldsymbol{X}^A,t)=\rho_0(\boldsymbol{X}^A,t)\ddot{\boldsymbol{u}}^A(\boldsymbol{x}^A,t),\\
&\quad\forall\mathbf{X}^A\in\Omega_0,\quad\mathbf{X}^B\in\mathcal{H}^A.
\end{aligned}\tag{50}$$

Proof We start with the proof of Eq. (49). The stress at point A is held constant in the integral in Eq. (46). This implies that the force state $\underline{\boldsymbol{T}}^{AB}$ is an odd function because the following condition is satisfied,

$$\underline{\boldsymbol{T}}^{AB}\langle\boldsymbol{\xi}^{AB}\rangle=-\underline{\boldsymbol{T}}^{AB}\langle-\boldsymbol{\xi}^{AB}\rangle.$$

If it is assumed that both the horizon and the influence function are symmetric, one can use the property shown above to show that

$$\int_{\mathcal{H}^A}\omega(\xi^{AB})\underline{\boldsymbol{T}}^{AB}\langle\boldsymbol{\xi}^{AB}\rangle\,dV^B=\boldsymbol{P}\left(\boldsymbol{x}^A,t\right)\cdot\boldsymbol{K}^{-1}(\boldsymbol{X}^A)\int_{\mathcal{H}^A}\omega(\xi^{AB})\boldsymbol{\xi}^{AB}\,dV^B=\mathbf{0},\tag{51}$$

as was assumed in deriving the convergence of the force state in Silling and Lehoucq [28]. Thus, if we replace the local divergence of the first Piola-Kirchhoff stress in Eq. (48) with the nonlocal material divergence, i.e. Eq. (42), Eq. (49) follows automatically.

Strictly speaking, Eq. (49) only holds when $\mathcal{H}^A\subset\Omega_0$. For uniform particle distribution and uniform horizon size, it is impossible to have this condition satisfied near the boundary of the domain, i.e. $dis\{\mathbf{X},\partial\Omega_0\}<\delta^A$. Therefore, in practical computation, we still recommend the following discrete dynamic equations as the governing equations of the total Lagrangian peridynamics formulation,

$$\begin{aligned}
\rho_0\ddot{\mathbf{u}}^A=&\sum_{B=1}^{N_{H_A}}\omega(\xi^{AB})\Big(\mathbf{P}(\mathbf{x}^B,t)-\mathbf{P}(\mathbf{x}^A,t)\Big)\\
&\times\mathbf{K}^{-1}(\mathbf{X}^A)\boldsymbol{\xi}^{AB}\Delta V^B\\
&+\mathbf{B}(\mathbf{X}^A,t),\quad A=1,2,\ldots,N.
\end{aligned}\tag{52}$$

Hence, one can readily show that the equation of motion (50) follows trivially by replacing the local divergence of the Piola-Kirchhoff stress in Eq. (48) with the nonlocal stress divergence defined in Eq. (44). The equation of motion using the force state expressed in Eqs. (43) and (45) will converge to the equation of motion of classical continuum mechanics as the horizon radius approaches zero if the horizon is a symmetric domain. This result is in agreement with the results in Silling and Lehoucq [28] where it was shown that the term involving force states in the peridynamics equation of motion converges to the stress divergence of classical continuum mechanics as the horizon approaches zero for any general elastic peridynamic material.

It is noted that the original generalized equation of motion in Silling et al. [26] includes the term $\underline{\boldsymbol{T}}^{AB}\langle\boldsymbol{\xi}^{AB}\rangle$, though this term is opposite in sign to the one presented in Eq. (42). In the case of a symmetric domain, both equations of motion are equivalent due to the antisymmetry of the expression in Eq. (51). Though the discrepancy between signs is insignificant in symmetric domains for Eq. (49), it retains significance in the stress divergence term that acts on the deformed bonds (Eq. (50)), because antisymmetry of the deformed bonds cannot generally be assumed. □

Proposition 3.8 *Given the relations between the nonlocal force state and the first Piola-Kirchhoff stress tensor* (Eq. (43) *with respect to the undeformed bond and Eq.* (45) *with respect to the deformed bond), the symmetric condition of the Cauchy stress tensor* $\boldsymbol{\sigma}$,

$$\boldsymbol{\sigma} = \boldsymbol{\sigma}^T,$$

implies the balance of the nonlocal angular momentum

$$\int_{\mathcal{H}^A} \omega(\xi^{AB}) \underline{\boldsymbol{T}}^{AB} \times \underline{\boldsymbol{Y}}^{AB}\, dV^B = \mathbf{0}, \quad \forall \mathbf{X}^B \in \mathcal{H}^A, \mathbf{X}^A \in \Omega_0 \tag{53}$$

at each point $\mathbf{X}^A \in \Omega_0$.

Proof The proof has two parts. First, using the force state that acts on the undeformed bonds, the nonlocal balance of angular momentum for each point $\mathbf{X}^A \in \Omega_0$ can be expressed in indicial notation as follows ([26]),

$$\begin{aligned}
&\int_{\mathcal{H}^A} \omega(\xi^{AB}) \underline{\boldsymbol{T}}^{AB} \langle \boldsymbol{\xi}^{AB} \rangle \times \underline{\boldsymbol{Y}}^{AB}\, dV^B \\
&\quad = e_{\ell ij} \int_{\mathcal{H}^A} \omega(\xi^{AB}) P^A_{iA} K^{-1}_{AB} \xi^{AB}_B \underline{Y}^{AB}_j\, dV^B \mathbf{E}_\ell \\
&\quad = e_{\ell ij} P^A_{iA} K^{-1}_{AB} N_{Bj} \mathbf{E}_\ell \\
&\quad = e_{\ell ij} P^A_{iA} F^T_{Aj} \langle \boldsymbol{\xi}^{AB} \rangle \mathbf{E}_\ell \\
&\quad = e_{\ell ij} \sigma^A_{ij} J \mathbf{E}_\ell \\
&\quad = \mathbf{0},
\end{aligned} \tag{54}$$

where lowercase and uppercase subscripts denote indices in the reference and current configuration, respectively, and $\mathbf{E}_\ell$ is the coordinate basis in the referential configuration.

In the above equation, we have used the relation $J\boldsymbol{\sigma} = \mathbf{P}\mathbf{F}^T$, where the Jacobian is defined as $J = det[\boldsymbol{F}]$ as it is defined in classical continuum mechanics. The last line of the above equation uses the property that the Cauchy stress tensor is symmetric.

Similarly, the nonlocal balance of angular momentum in terms of the force state acting on the deformed bonds is expressed as

$$\begin{aligned}
&\int_{\mathcal{H}^A} \omega(\xi^{AB}) \underline{\boldsymbol{T}}^{AB} \langle \underline{\boldsymbol{Y}}^{AB} \rangle \times \underline{\boldsymbol{Y}}^{AB}\, dV^B \\
&\quad = e_{\ell ik} \int_{\mathcal{H}^A} \omega(\xi^{AB}) P^A_{iA} N^{-1}_{Aj} \underline{Y}^{AB}_j \underline{Y}^{AB}_k\, dV^B \mathbf{E}_\ell \\
&\quad = e_{\ell ik} P^A_{iA} N^{-1}_{Aj} M_{jk} \mathbf{E}_\ell \\
&\quad = e_{\ell ik} P^A_{iA} F_{Ak} \langle \underline{\boldsymbol{Y}}^{AB} \rangle \mathbf{E}_\ell \\
&\quad = e_{\ell ik} \sigma^A_{ik} J \mathbf{E}_\ell \\
&\quad = \mathbf{0}.
\end{aligned} \tag{55}$$

In passing, we note that the nonlocal global balance of angular momentum is expressed formally, $\forall \mathbf{X}^A \in \Omega_0$,

$$\begin{aligned}
&\int_{\mathcal{H}^A} \left(\mathcal{M}_X\left[\boldsymbol{P}(\boldsymbol{x}^A, t) \right] + \boldsymbol{B}(\boldsymbol{X}^A, t) \right) \times \underline{\boldsymbol{Y}}^{AB}\, dV^A \\
&\quad = \int_{\mathcal{H}^A} \rho_0(\boldsymbol{X}^A) \ddot{\boldsymbol{u}}(\boldsymbol{X}^A, t) \times \underline{\boldsymbol{Y}}^{AB}\, dV^A.
\end{aligned} \tag{56}$$

The nonlocal stress divergence term also involves the stress at point B, which is a function of the variable dV^B. Therefore, angular momentum using $\underline{\boldsymbol{T}}^{BA}$ will not result in the same balance as expressed in Eqs. (54) and (55). We have proved that in the limit of an infinitesimal horizon, the balance of linear momentum (as well as the stress divergence term) will approach the value of their classical continuum mechanics counterparts. Therefore, with the assumption that the cauchy stress tensor is symmetric, Eq. (56) will also be valid in the limit of an infinitesimal horizon. □

3.2 Updated Lagrangian approach

For the updated Lagrangian approach, the equations of motion are formulated in the current configuration, which is assumed to be the new reference configuration. Thus the updated Lagrangian formulation uses spatial derivatives that are defined as the derivative with respect to the current configuration of a deformed body. Based on this approach, we propose the following nonlocal equivalent of a spatial gradient:

Definition 3.2 *(Nonlocal Spatial Differential Operators)* For any N-dimensional composite field function $\hat{G}(\boldsymbol{x}) := (G \circ \boldsymbol{x})(\boldsymbol{X}) = G[\boldsymbol{x}(\boldsymbol{X})]$, $\hat{G}(\boldsymbol{x}) \in \mathbb{R}^{n_i \times \ldots n_N}, n_i \in \mathbb{Z}^+$ defined at point A that satisfies the following properties:

1. Locally analytic at points A;
2. Integrable within the entire horizon $\mathcal{H}^A(t)$, and
3. Contain a set of symmetric horizons that provides a cover for the physical spatial domain Ω_t.

The nonlocal spatial gradient as a function of the undeformed bonds is expressed as

$$\begin{aligned}
&\hat{\mathcal{L}}_x\left[\hat{G}(\boldsymbol{x}) \right]\left(< \boldsymbol{\xi}^{AB} >_x \right) \\
&\quad := \left[\int_{\mathcal{H}^A(t)} \omega_t(Y^{AB})\, \Delta\hat{G}(\boldsymbol{x}) \otimes \boldsymbol{\xi}^{AB}\, dv^B \right] \mathbf{N}^{-1}\left(\boldsymbol{x}, \boldsymbol{X}^A \right),
\end{aligned} \tag{57}$$

where $Y^{AB} = \|\mathbf{Y}^{AB}\|_2$, and $\mathbf{N}$ is the two-point correlation tensor.

The nonlocal spatial gradient of $\hat{G}(\boldsymbol{x})$ is defined as a function of the deformed bonds at point A as

$$\hat{\mathcal{L}}_x[\hat{G}(\boldsymbol{x})](< \underline{\boldsymbol{Y}}^{AB} >_x) := \left[\int_{\mathcal{H}^A(t)} \omega_t(Y^{AB})\, \Delta\hat{G}(\boldsymbol{x}) \otimes \underline{\boldsymbol{Y}}^{AB}\, dv^B\right]\mathbf{M}^{-1}(\boldsymbol{x}^A), \tag{58}$$

where $\mathbf{M}$ is the shape tensor for the spatial horizon.

The nonlocal spatial divergence operator is constructed in a similar fashion as an implicit function of the average undeformed bonds

$$\hat{\mathcal{M}}_x[\hat{G}(\boldsymbol{x}^A)](< \boldsymbol{\xi}^{AB} >_x) := \int_{\mathcal{H}^A(t)} \omega_t(Y^{AB})\Delta\hat{G}(\boldsymbol{x}) \cdot \left(\mathbf{N}^{-T}(\boldsymbol{x}^A, \boldsymbol{X}^A)\boldsymbol{\xi}^{AB}\right) dv^B, \tag{59}$$

and likewise as an implicit function of the average deformed bonds

$$\hat{\mathcal{M}}_x[\hat{G}(\boldsymbol{x}^A)](< \mathbf{Y}^{AB} >_x) := \int_{\mathcal{H}^A(t)} \omega_t(Y^{AB})\Delta\hat{G}(\boldsymbol{x}) \cdot \left(\mathbf{M}^{-1}(\boldsymbol{x}^A)\mathbf{Y}^{AB}\right) dv^B \tag{60}$$

where $\omega_t(Y^{AB}) = J^{-1}\omega(\xi^{AB})$.

The variable of integration in the nonlocal spatial gradient and divergence operators is based on the coordinates in the current configuration, notated as dv^B. The bounds of integration are on the deformed horizon at time t denoted as $\mathcal{H}^A(t)$. Note that the variable of integration in the current configuration is related to the variables in the reference configuration via the Jacobian $dv^B \equiv JdV^B = det[\boldsymbol{F}]dV^B$. The Jacobian is assumed to be constant because the deformation gradient is constant throughout the horizon as well. This assumption ensures the symmetry of the integration domain in the current configuration.

The mathematical meaning of the definition of a nonlocal spatial gradient operator may be understood as,

$$\nabla_x \otimes \left(\bullet\right) \rightarrow \frac{1}{\Delta\mathbf{x}}\left(\Delta(\bullet)\right) := \left[\int_{\mathcal{H}^A(t)} \omega_t(Y^{AB}) \left(\Delta(\bullet)\right) \otimes \boldsymbol{Y}^{AB}\, dv^B\right]\boldsymbol{M}^{-1}. \tag{61}$$

Following the same notation, we can understand the nonlocal spatial divergence operator as

$$\nabla_x \cdot \left(\bullet\right) \rightarrow \mathrm{Tr}\left(\frac{1}{\Delta\mathbf{x}}\left(\Delta(\bullet)\right)\right) := \left[\int_{\mathcal{H}^A(t)} \omega_t(Y^{AB}) \left(\Delta(\bullet)\right) \cdot \boldsymbol{Y}^{AB}\, dv^B\right]\boldsymbol{M}^{-1}. \tag{62}$$

Since $\boldsymbol{M}^{-1}$ is symmetric, Eq. (62) can be rewritten as

$$\int_{\mathcal{H}^A(t)} \omega(Y^{AB}) \left(\Delta(\bullet)\right) \cdot (\boldsymbol{M}^{-1}\mathbf{Y}^{AB})\, dv^B. \tag{63}$$

These nonlocal operators share the same properties as their nonlocal material counterparts presented in the previous section, as will be shown below.

Theorem 3.9 *The nonlocal spatial gradient operators defined in Eqs. (57) and (58) converge to the localized gradient operator as the horizon radius approaches zero,*

$$\lim_{\delta^A \to 0} \hat{\mathcal{L}}_x[\hat{G}(\boldsymbol{x}^A)] = \left[\nabla_x \hat{G}(\boldsymbol{x})\right]_{\boldsymbol{x}=\boldsymbol{x}^A}. \tag{64}$$

Proof By using Eq. (57), the proof follows a similar procedure as was done in proving the convergence of Eq. (10). Expanding $\hat{G}(\boldsymbol{x})$ at point A via Taylor series, we have

$$\hat{G}(\boldsymbol{x}) = \hat{G}(\boldsymbol{x}^A) + \left[\nabla_x \hat{G}(\boldsymbol{x})\right]_{\boldsymbol{x}=\boldsymbol{x}^A} \cdot (\boldsymbol{x} - \boldsymbol{x}^A) + \mathcal{O}\left(\|\boldsymbol{x} - \boldsymbol{x}^A\|_2^2\right) \tag{65}$$

Substituting $\boldsymbol{x}$ with $\boldsymbol{x}^B$ yields,

$$\Delta\hat{G}(\boldsymbol{x}) = \hat{G}(\boldsymbol{x}^B) - \hat{G}(\boldsymbol{x}^A) = \left[\nabla_x \hat{G}(\boldsymbol{x})\right]_{\boldsymbol{x}=\boldsymbol{x}^A} \cdot \underline{\boldsymbol{Y}}^{AB} + \mathcal{O}\left(\|\underline{\boldsymbol{Y}}^{AB}\|_2^2\right) \tag{66}$$

Inserting the finite difference $\Delta\hat{G}(\boldsymbol{x})$ into the nonlocal differential operator in Eq. (57),

$$\begin{aligned}\hat{\mathcal{L}}_X[G(\boldsymbol{X}^A)](< \boldsymbol{Y}^{AB} >_X) &= \left[\left(\left[\nabla_x \hat{G}(\boldsymbol{x})\right]_{\boldsymbol{x}=\boldsymbol{x}^A} \cdot \underline{\boldsymbol{Y}}^{AB} + \mathcal{O}(\|\underline{\boldsymbol{Y}}^{AB}\|_2^2)\right) \hat{\circledast} \boldsymbol{\xi}^{AB}\right]\mathbf{N}^{-1} \\ &= \left[\nabla_x \hat{G}(\boldsymbol{x})\right]_{\boldsymbol{x}=\boldsymbol{x}^A} + \left[\mathcal{O}(\|\underline{\boldsymbol{Y}}^{AB}\|_2^2)\right] \hat{\circledast} \boldsymbol{\xi}^{AB}\mathbf{N}^{-1}\end{aligned} \tag{67}$$

where the operator $\hat{\circledast}$ is defined as

$$\boldsymbol{U} \hat{\circledast} \boldsymbol{V} := \int_{\mathcal{H}^A(t)} \omega_t(Y^{AB})\, \boldsymbol{U} \otimes \boldsymbol{V}\, dv^B, \quad (\boldsymbol{U}, \boldsymbol{V}) \in \mathbb{R}^3$$

$$\boldsymbol{U} \hat{\bullet} \boldsymbol{V} := \int_{\mathcal{H}^A(t)} \omega_t(Y^{AB})\, \boldsymbol{U} \cdot \boldsymbol{V}\, dv^B, \quad (\boldsymbol{U}, \boldsymbol{V}) \in \mathbb{R}^3.$$

Following the same assumption of the last section, the leading remainder is of order $\mathcal{O}(||\mathbf{Y}^{AB}||_2^2)$.

A similar calculation can be carried out for the gradient operator in Eq. (58) by swapping the differential operators. The remainder will vanishes as the horizon radius approaches zero. □

Theorem 3.10 *The nonlocal spatial divergence operators defined in Eqs.* (59) *and* (60) *converge to the localized gradient operator as the horizon radius approaches zero.*

$$\lim_{\delta^A \to 0} \hat{\mathcal{M}}_x[G(\boldsymbol{x}^A)] = \left[\nabla_x \cdot G(\boldsymbol{x})\right]_{\boldsymbol{x}=\boldsymbol{x}^A} \tag{68}$$

Proof Inserting the exact difference $\Delta\hat{G}(\boldsymbol{x})$ into the spatial divergence operator that acts on the undeformed bonds, we obtain the following expression,

$$\begin{aligned}\hat{\mathcal{M}}_x[\hat{G}(\boldsymbol{x}^A)](<\boldsymbol{\xi}^{AB}>_x) &= \left[\left(\left[\nabla_x \hat{G}(\boldsymbol{x})\right]_{\boldsymbol{x}=\boldsymbol{x}^A} \cdot \underline{\boldsymbol{Y}}^{AB} + \mathcal{O}(\|\underline{\boldsymbol{Y}}^{AB}\|_2^2)\right)\hat{\bullet}\mathbf{N}^{-T}\boldsymbol{\xi}^{AB}\right] \\ &= \left[\nabla_x \hat{G}(\boldsymbol{x})\right]_{\boldsymbol{x}=\boldsymbol{x}^A} : \boldsymbol{I} + \left(\mathcal{O}(\|\underline{\boldsymbol{Y}}^{AB}\|_2^2)\right)\hat{\bullet}\mathbf{N}^{-T}\boldsymbol{\xi}^{AB} \\ &= \left[\nabla_x \cdot \hat{G}(\boldsymbol{x})\right]_{\boldsymbol{x}=\boldsymbol{x}^A} + \left(\mathcal{O}(\|\underline{\boldsymbol{Y}}^{AB}\|_2^2)\right)\hat{\bullet}\mathbf{N}^{-T}\boldsymbol{\xi}^{AB}.\end{aligned} \tag{69}$$

Similarly, inserting the exact difference into the spatial divergence operator that acts on the deformed bonds, we have,

$$\begin{aligned}\hat{\mathcal{M}}_x[\hat{G}(\boldsymbol{x}^A)](<\boldsymbol{\xi}^{AB}>_x) &= \left[\left(\left[\nabla_x \hat{G}(\boldsymbol{x})\right]_{\boldsymbol{x}=\boldsymbol{x}^A} \cdot \underline{\boldsymbol{Y}}^{AB} + \mathcal{O}(\|\underline{\boldsymbol{Y}}^{AB}\|_2^2)\right)\hat{\bullet}\mathbf{M}^{-1}\underline{\boldsymbol{Y}}^{AB}\right] \\ &= \left[\nabla_x \hat{G}(\boldsymbol{x})\right]_{\boldsymbol{x}=\boldsymbol{x}^A} : \boldsymbol{I} + \left(\mathcal{O}(\|\underline{\boldsymbol{Y}}^{AB}\|_2^2)\right)\hat{\bullet}\mathbf{M}^{-1}\underline{\boldsymbol{Y}}^{AB} \\ &= \left[\nabla_x \cdot \hat{G}(\boldsymbol{x})\right]_{\boldsymbol{x}=\boldsymbol{x}^A} + \left(\mathcal{O}(\|\underline{\boldsymbol{Y}}^{AB}\|_2^2)\right)\hat{\bullet}\mathbf{M}^{-1}\underline{\boldsymbol{Y}}^{AB}.\end{aligned} \tag{70}$$

Using the antisymmetry condition of the integral of the highest order remainder term, the resulting truncation error of the nonlocal spatial divergence operators is $\mathcal{O}(||\mathbf{Y}^{AB}||_2^2)$, which converges to zero in the limit as the horizon radius approaches zero. □

3.3 Nonlocal spatial gradient as the inverse of deformation gradient

Comparing with the nonlinear continuum mechanics [16], we may use the nonlocal spatial gradient operator to define the inverse of the deformation gradient,

$$\begin{aligned}\boldsymbol{\mathcal{F}}^{-1} &:= \frac{\partial \mathbf{X}}{\partial \mathbf{x}} \leftrightarrow \hat{\mathbf{F}}_A^{-1} := \mathbf{N}^T \boldsymbol{M}^{-1} \\ &= \left(\int_{\mathcal{H}_t^A} \omega_t(Y^{AB})\boldsymbol{\xi}^{AB} \otimes \mathbf{Y}^{AB} dv^B\right)\boldsymbol{M}^{-1}.\end{aligned} \tag{71}$$

Moreover, from Eq. (33), one can clearly see that

$$\left(\hat{\mathbf{F}}_A^{-1}\right)^{-1} = \left(\mathbf{N}^T\mathbf{M}^{-1}\right)^{-1} = \mathbf{M}\mathbf{N}^{-T} = \hat{\mathbf{F}}_A.$$

On the other hand, Assume that inside the horizon $\mathcal{H}^A$ the Cauchy-Born rule applies, i.e.

$$\boldsymbol{\xi}^{AB} = \boldsymbol{\mathcal{F}}_A^{-1}(t)\mathbf{Y}^{AB}(t). \tag{72}$$

Substituting (71) into (72) yields,

$$\hat{\mathbf{F}}_A^{-1} = \boldsymbol{\mathcal{F}}_A^{-1}(t) \quad \rightarrow \quad \hat{\mathbf{F}}_A^{-1} = \mathbf{F}_A^{-1},$$

by virtue of Eq. (40).

3.3.1 Nonlocal divergence of spatial stress distribution

In the updated Lagrangian approach, the equation of motion is formulated entirely in the current configuration of a deformed nonlocal medium,

$$\nabla_x \cdot \boldsymbol{\sigma}(\boldsymbol{x}, t) + \boldsymbol{b}(\boldsymbol{x}, t) = \rho(\boldsymbol{x}, t)\ddot{\boldsymbol{u}}(\boldsymbol{x}, t) \tag{73}$$

where $\boldsymbol{\sigma}$ is the Cauchy stress tensor defined as the force per unit area in the current configuration. $\boldsymbol{b}$ and ρ are defined as the body force and density in the current configuration.

The nonlocal equivalent to the spatial stress divergence in Eq. (73) is presented in the following proposition.

Proposition 3.11 *Given a point* $\mathbf{x}^A \in \Omega(t)$ *and neighbors* $\mathbf{x}^B \in \mathcal{H}^A(t)$ *that contain a non-zero stress and satisfy the conditions of Definition* 3.2*, the nonlocal spatial divergence of the Cauchy stress tensor is expressed as a function of the undeformed bonds as*

$$\begin{aligned}&\hat{\mathcal{M}}_x[\boldsymbol{\sigma}(\boldsymbol{x}^A, t)](<\boldsymbol{\xi}^{AB}>_x) \\ &= -\int_{\mathcal{H}^A(t)} \omega(\xi^{AB})\left(\underline{\boldsymbol{T}}_\sigma^{AB}\langle\boldsymbol{\xi}^{AB}\rangle + \underline{\boldsymbol{T}}_\sigma^{BA}\langle\boldsymbol{\xi}^{BA}\rangle\right) dv^B\end{aligned} \tag{74}$$

where the force states as functions of the Cauchy stress acting on particle A and B are defined as

$$\begin{aligned}\underline{\boldsymbol{T}}_\sigma^{AB}[\boldsymbol{x}^A, t]\langle\boldsymbol{\xi}^{AB}\rangle &= \boldsymbol{\sigma}\left(\boldsymbol{x}^A, t\right) \cdot \boldsymbol{N}^{-T}\left(\boldsymbol{x}^A, \boldsymbol{X}^A\right)\boldsymbol{\xi}^{AB} \\ \underline{\boldsymbol{T}}_\sigma^{BA}[\boldsymbol{x}^B, t]\langle\boldsymbol{\xi}^{BA}\rangle &= \boldsymbol{\sigma}\left(\boldsymbol{x}^B, t\right) \cdot \boldsymbol{N}^{-T}\left(\boldsymbol{x}^A, \boldsymbol{X}^A\right)\boldsymbol{\xi}^{BA}\end{aligned} \tag{75}$$

The spatial divergence as a function of the deformed bonds is expressed as

$$\begin{aligned}&\hat{\mathcal{M}}_x[\boldsymbol{\sigma}(\boldsymbol{x}^A, t)](<\mathbf{Y}^{AB}>_x) \\ &= -\int_{\mathcal{H}^A(t)} \omega(\xi^{AB})\left(\underline{\boldsymbol{T}}_\sigma^{AB}\langle\underline{\boldsymbol{Y}}^{AB}\rangle + \underline{\boldsymbol{T}}_\sigma^{BA}\langle\underline{\boldsymbol{Y}}^{BA}\rangle\right) dv^B\end{aligned} \tag{76}$$

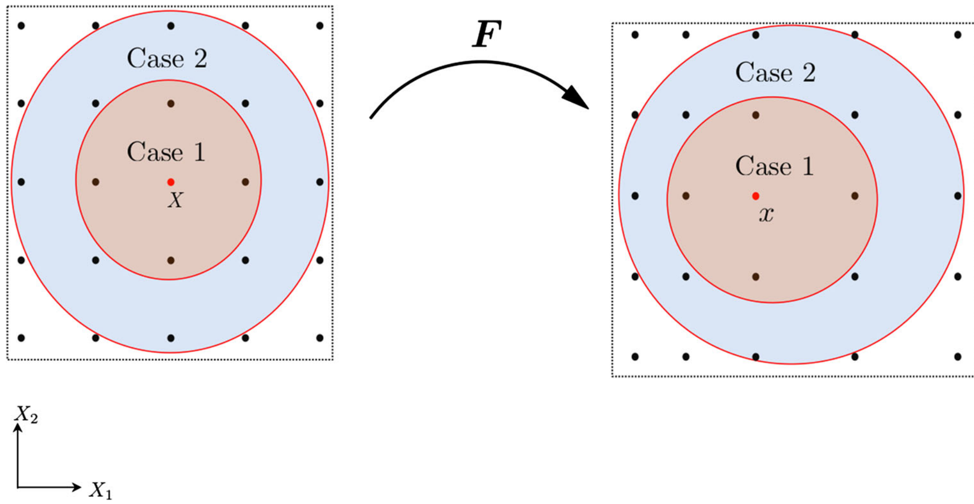

Fig. 5 2D Discretized domain of particles subjected to a non-linear 1D deformation along the X_1 axis

where the force states introduced above are defined as:

$$\underline{\boldsymbol{T}}_{\sigma}^{AB}[\boldsymbol{x}^A, t]\langle \underline{\boldsymbol{Y}}^{AB}\rangle = \boldsymbol{\sigma}(\boldsymbol{x}^A, t) \cdot \boldsymbol{M}^{-1}(\boldsymbol{x}^A)\underline{\boldsymbol{Y}}^{AB}$$
$$\underline{\boldsymbol{T}}_{\sigma}^{BA}[\boldsymbol{x}^B, t]\langle \underline{\boldsymbol{Y}}^{BA}\rangle = \boldsymbol{\sigma}(\boldsymbol{x}^B, t) \cdot \boldsymbol{M}^{-1}(\boldsymbol{x}^A)\underline{\boldsymbol{Y}}^{BA} \tag{77}$$

Proof The spatial divergence of the Cauchy stress tensor in terms of the undeformed bonds can be derived by using the nonlocal differential operator in Eq. (59) as follows,

$$\begin{aligned} &\hat{\mathcal{M}}_x[\boldsymbol{\sigma}(\boldsymbol{x}^A, t)](<\boldsymbol{\xi}^{AB}>_x) \\ &= \int_{\mathcal{H}^A(t)} \omega_t(Y^{AB})\Delta\boldsymbol{\sigma}(\boldsymbol{x}, t) \cdot \left(\boldsymbol{N}^{-T}(\boldsymbol{x}^A, \boldsymbol{X}^A)\boldsymbol{\xi}^{AB}\right) dv^B \\ &= \int_{\mathcal{H}^A(t)} \omega_t(Y^{AB})\left(\boldsymbol{\sigma}(\boldsymbol{x}^B, t) - \boldsymbol{\sigma}(\boldsymbol{x}^A, t)\right) \\ &\quad \times \left(\boldsymbol{N}^{-T}(\boldsymbol{x}^A, \boldsymbol{X}^A)\boldsymbol{\xi}^{AB}\right) dv^B \\ &= -\int_{\mathcal{H}^A(t)} \omega_t(Y^{AB})\left(\underline{\boldsymbol{T}}_{\sigma}^{AB}\langle\boldsymbol{\xi}^{AB}\rangle + \underline{\boldsymbol{T}}_{\sigma}^{BA}\langle\boldsymbol{\xi}^{BA}\rangle\right) dv^B. \end{aligned} \tag{78}$$

The spatial stress divergence in terms of the deformed bonds is formulated through the use of Eq. (60),

$$\begin{aligned} &\hat{\mathcal{M}}_x[\boldsymbol{\sigma}(\boldsymbol{x}^A, t)](<\boldsymbol{\xi}^{AB}>_x) \\ &= \int_{\mathcal{H}^A(t)} \omega_t(Y^{AB})\Delta\boldsymbol{\sigma}(\boldsymbol{x}, t) \cdot \left(\boldsymbol{M}^{-1}(\boldsymbol{x}^A)\underline{\boldsymbol{Y}}^{AB}\right) dv^B \\ &= \int_{\mathcal{H}^A(t)} \omega_t(Y^{AB})\left(\boldsymbol{\sigma}(\boldsymbol{x}^B, t) - \boldsymbol{\sigma}(\boldsymbol{x}^A, t)\right) \\ &\quad \cdot \left(\boldsymbol{M}^{-1}(\boldsymbol{x}^A)\underline{\boldsymbol{Y}}^{AB}\right) dv^B \\ &= -\int_{\mathcal{H}^A(t)} \omega_t(Y^{AB})\left(\underline{\boldsymbol{T}}_{\sigma}^{AB}\langle\underline{\boldsymbol{Y}}^{AB}\rangle + \underline{\boldsymbol{T}}_{\sigma}^{BA}\langle\underline{\boldsymbol{Y}}^{BA}\rangle\right) dv^B. \end{aligned} \tag{79}$$

□

Proposition 3.12 *Given that balance of linear momentum is locally satisfied for each point A in the spatial domain* Ω

$$\int_{\Omega} \left[\nabla_{\boldsymbol{x}} \cdot \boldsymbol{\sigma}(\boldsymbol{x}^A, t) + \boldsymbol{b}(\boldsymbol{x}^A, t)\right] dv = \int_{\Omega} \rho(\boldsymbol{x}^A, t)\ddot{\boldsymbol{u}}(\boldsymbol{x}^A, t)\, dv, \quad \forall \mathbf{x}^A \in \Omega(t) \in \Omega \tag{80}$$

the nonlocal balance of linear momentum will also be satisfied in the limit as the horizon radius approaches zero, thus yielding the equation of motion for each point A given as a function of the undeformed bonds expressed as

$$-\int_{\mathcal{H}^A(t)} \omega_t(Y^{AB})\left(\underline{\mathbf{T}}_{\sigma}^{AB}\langle\boldsymbol{\xi}^{AB}\rangle + \underline{\boldsymbol{T}}_{\sigma}^{BA}\langle\boldsymbol{\xi}^{BA}\rangle\right)dv^B + \boldsymbol{b}(\boldsymbol{x}^A, t) = \rho(\boldsymbol{x}^A, t)\ddot{\boldsymbol{u}}(\boldsymbol{x}^A, t). \tag{81}$$

Alternatively, it may be expressed as a function of the deformed bonds as

$$-\int_{\mathcal{H}^A(t)} \omega_t(Y^{AB})\underline{\boldsymbol{T}}_{\sigma}^{BA}\langle\underline{\boldsymbol{Y}}^{BA}\rangle)\, dv^B + \boldsymbol{b}(\boldsymbol{x}^A, t) = \rho(\boldsymbol{x}^A, t)\ddot{\boldsymbol{u}}(\boldsymbol{x}^A, t). \tag{82}$$

Proof In the updated Lagrangian approach, Eq. (81) is obtained by replacing the local stress divergence in Eq. (73) with its nonlocal counterpart in Eq. (74). Noting that because in the updated Lagrangian approach, the horizon $\mathcal{H}^A(t)$ is constructed in a symmetric shape, thus the shape of $\mathcal{H}(0)$ is not symmetric nor isotropic in general. Therefore, in general

$$\int_{\mathcal{H}^A(t)} \omega_t(Y^{AB})\underline{\mathbf{T}}_{\sigma}^{AB}\langle\boldsymbol{\xi}^{AB}\rangle dv^B = \int_{\mathcal{H}_0^A} \omega_t(\xi^{AB})\underline{\mathbf{T}}_{\sigma}^{AB}\langle\boldsymbol{\xi}^{AB}\rangle dV^B \neq 0\,!$$

On the other hand, since $\mathcal{H}^A(t)$ is symmetric,

$$\int_{\mathcal{H}^A(t)} \underline{\boldsymbol{T}}_{\sigma}^{AB}\langle \underline{\mathbf{Y}}^{AB}\rangle dv^B = \boldsymbol{\sigma}(\mathbf{x}^A, t)\mathbf{M}^{-1}(\mathbf{x}^A)\int_{\mathcal{H}^A(t)} \underline{\mathbf{Y}}^{AB} dv^B = 0, \tag{83}$$

because the first moment of a symmetric shape vanishes. Thus, we can eliminate this term as mentioned in Eq. (79). Subsequently, Eq. (82) is also obtained by replacing the local stress divergence with its nonlocal counterpart,

In the current configuration, the particle positions are constantly changing. Even though the horizon shape is symmetric, the changing particle distribution cannot maintain a symmetric distribution. Thus the discretized version of Eq. (83) cannot be hold. In practical computation, we still recommend to use the following updated Lagrangian peridynamics equation of motion,

$$\rho_t^A \ddot{\mathbf{u}}_A = \sum_{B=1}^{N_{H_A}} \omega(\xi^{AB})\left(\boldsymbol{\sigma}^B - \boldsymbol{\sigma}^A\right)\cdot \mathbf{M}^{-1}(\mathbf{x}^A)\boldsymbol{\xi}^{AB}\Delta V^B + \mathbf{b}(\mathbf{x}^A, t). \tag{84}$$

□

Proposition 3.13 *Given the nonlocal spatial divergence of the Cauchy stress tensor given by Eqs. (74) and (76), and assuming the symmetry of the Cauchy stress tensor,*

$$\boldsymbol{\sigma} = \boldsymbol{\sigma}^T,$$

the nonlocal balance of angular momentum expressed as

$$\int_{\mathcal{H}^A(t)} \omega_t(Y^{AB})\underline{\boldsymbol{T}}_{\boldsymbol{\sigma}}^{AB} \times \underline{\boldsymbol{Y}}^{AB} dv^B = \mathbf{0}, \quad \forall \mathbf{x}^B \in \mathcal{H}^A, \mathbf{x}^A \in \Omega, \tag{85}$$

which is satisfied for each point $\mathbf{x}^A$ in the spatial domain Ω.

Proof We begin by analyzing the stress divergence in Eq. (74). The balance of angular momentum is formulated as follows

$$\begin{aligned}
&\int_{\mathcal{H}^A(t)} \omega_t(Y^{AB})\underline{\boldsymbol{T}}_{\sigma}^{AB}\langle \boldsymbol{\xi}^{AB}\rangle \times \underline{\boldsymbol{Y}}^{AB}\, dv^B \\
&= e_{\ell ik}\int_{\mathcal{H}^A(t)} \omega_t(Y^{AB})\sigma_{ij}^A N_{jA}^{-1}\xi_A^{AB} Y_k^{AB}\, dv^B \mathbf{e}_\ell \\
&= e_{\ell ik}\sigma_{ij}^A N_{jA}^{-1} N_{Ak} \boldsymbol{J}\mathbf{e}_\ell \\
&= e_{\ell ik}\sigma_{ij}^A \delta_{jk} \boldsymbol{J}\mathbf{e}_\ell \\
&= e_{\ell ik}\sigma_{ik}^A \boldsymbol{J}\mathbf{e}_\ell \\
&= \mathbf{0}.
\end{aligned} \tag{86}$$

Table 1 Nonlocal field variables in different configuration spaces

Deformation gradient	$\boldsymbol{F}\langle\xi\rangle = \boldsymbol{N}\boldsymbol{K}^{-1}$	$\boldsymbol{F}\langle\underline{Y}\rangle = \boldsymbol{M}\boldsymbol{N}^{-T}$
Total Lagrangian stress divergence	$\underline{\boldsymbol{T}}\langle\xi\rangle = \boldsymbol{P}\boldsymbol{K}^{-1}\boldsymbol{\xi}$	$\underline{\boldsymbol{T}}\langle\underline{Y}\rangle = \boldsymbol{P}\boldsymbol{N}^{-1}\underline{\boldsymbol{Y}}$
Updated Lagrangian stress divergence	$\underline{\boldsymbol{T}}_{\sigma}\langle\xi\rangle = \boldsymbol{\sigma}\boldsymbol{N}^{-T}\boldsymbol{\xi}$	$\underline{\boldsymbol{T}}_{\sigma}\langle\underline{Y}\rangle = \boldsymbol{\sigma}\boldsymbol{M}^{-1}\underline{\boldsymbol{Y}}$

where $\mathbf{e}_\ell$ is the basis vector of the coordinate in the current configuration.

The angular momentum balance using the stress divergence as a function of the deformed bonds is expressed as

$$\begin{aligned}
&\int_{\mathcal{H}^A(t)} \omega_t(Y^{AB})\underline{\boldsymbol{T}}_{\sigma}^{AB}\langle \underline{\boldsymbol{Y}}^{AB}\rangle \times \underline{\boldsymbol{Y}}^{AB}\, dv^B \\
&= e_{\ell im}\int_{\mathcal{H}^A(t)} \omega_t(Y^{AB})\sigma_{ij}^A M_{jk}^{-1} Y_k^{AB} Y_m^{AB}\, dv^B \mathbf{e}_\ell \\
&= e_{\ell im}\sigma_{ij}^A M_{jk}^{-1} M_{km} \boldsymbol{J}\mathbf{e}_\ell \\
&= e_{\ell im}\sigma_{ij}^A \delta_{jm} \boldsymbol{J}\mathbf{e}_\ell \\
&= e_{\ell im}\sigma_{im}^A \boldsymbol{J}\mathbf{e}_\ell \\
&= \mathbf{0}.
\end{aligned} \tag{87}$$

□

We summarize the nonlocal field variables derived in this paper in the following Table 1.

The updated Lagrangian approach essentially treats its current configuration as a "new" reference configuration, thus updating each variable with time. This is in contrast to the total lagrangian whereby the reference configuration is fixed based on the initial positions $\boldsymbol{X}$ and only updates the time-dependent variables. As will be shown in the next section, the nonlocal total and updated lagrangian equations of motion both yield identical values, and hence, identical convergence rates.

4 Numerical examples

In this Section, we present two numerical examples. The first example is a fundamental study that examines the convergence rate of the nonlocal equations of motion and deformation gradients to their local counterparts in classical continuum mechanics. In the second example, we employ both the total Lagrangian peridynamics approach and the updated Lagrangian peridynamics approach to simulate a uniaxial tension of three-dimensional hyperelastic bar.

4.1 Numerical example I: convergence of the nonlocal differential operators

We consider a 2D domain consisting of a meshless grid of particles that are evenly spaced in increments denoted as

Table 2 Convergence test cases

Case	Horizon radius	Variables
1a	ΔX	$\boldsymbol{F}\langle\boldsymbol{\xi}\rangle, \underline{\boldsymbol{T}}\langle\boldsymbol{\xi}\rangle, J\underline{\boldsymbol{T}}_\sigma\langle\boldsymbol{\xi}\rangle$
1b	ΔX	$\boldsymbol{F}\langle\underline{\boldsymbol{Y}}\rangle, \underline{\boldsymbol{T}}\langle\underline{\boldsymbol{Y}}\rangle, J\underline{\boldsymbol{T}}_\sigma\langle\underline{\boldsymbol{Y}}\rangle$
2a	$2\Delta X$	$\boldsymbol{F}\langle\boldsymbol{\xi}\rangle, \underline{\boldsymbol{T}}\langle\boldsymbol{\xi}\rangle, J\underline{\boldsymbol{T}}_\sigma\langle\boldsymbol{\xi}\rangle$
2b	$2\Delta X$	$\boldsymbol{F}\langle\underline{\boldsymbol{Y}}\rangle, \underline{\boldsymbol{T}}\langle\underline{\boldsymbol{Y}}\rangle, J\underline{\boldsymbol{T}}_\sigma\langle\underline{\boldsymbol{Y}}\rangle$

ΔX. Since the field variables are defined at the particle coordinates, each integral expression is only analyzed at these discrete points. Therefore, integrals are evaluated as finite sums over the set of all particle points within the integration bounds

$$\int_{\mathcal{H}^A} (\bullet)\, dV^B = \sum_{B\in\mathcal{H}^A} (\bullet)\, \Delta V^B,$$

where the equality holds when the nodal integration is exact. We consider a linear elastic constitutive model with Lamé parameters of $\lambda = 100$ and $\mu = 50$. In addition, the deformation is imposed on all of the particles via the nonlinear mapping of the following form

$$x_1 = (X_1)^4$$
$$x_2 = X_2 \qquad (88)$$

The convergence of the deformation gradient and force state will be analyzed assuming that the grid spacing ΔX is decreased at the same rate as the horizon radius δ. We examine the convergence by varying the horizon radius using the cases listed in Table 2.

The configuration of the mapping for each case is depicted in Fig. 9.

As shown in Fig. 6, the convergence slope for all cases in the L_∞-norm exhibits a second order accuracy. Therefore, as the horizon radius approaches zero, the nonlocal measures approach their localized counterparts at a rate of δ^2. The nonlocal material stress divergence and the nonlocal spatial stress divergence factored by the Jacobian nearly match in value for each subcase. This illustrates that the nonlocal total and updated lagrangian approaches are equivalent, as they are in classical continuum mechanics. In case 2, the horizon contains more neighbors and thus incorporates a higher level of nonlocality. These cases are shown to converge consistently to the classical continuum mechanics values at the same rate as case 1. However, the magnitude of the errors in case 2 are higher than their counterparts in case 1 by a constant. It is noted that only interior portions of the domain are included in the convergence study, because boundary particles will contain additional errors due to particle deficiencies within the horizon. Errors due to particle deficiencies is a known issue that is addressed in various literature, notably [19] in the context of particle methods and [8] in the context of nonlocal differential operators. For illustrative purposes, we show the "finest" nonlocal stress divergence (from case 1), as well as the classical continuum mechanics values in Fig. 7. Figure 8 shows the exact values of the stresses, which match with both cases 1 and 2.

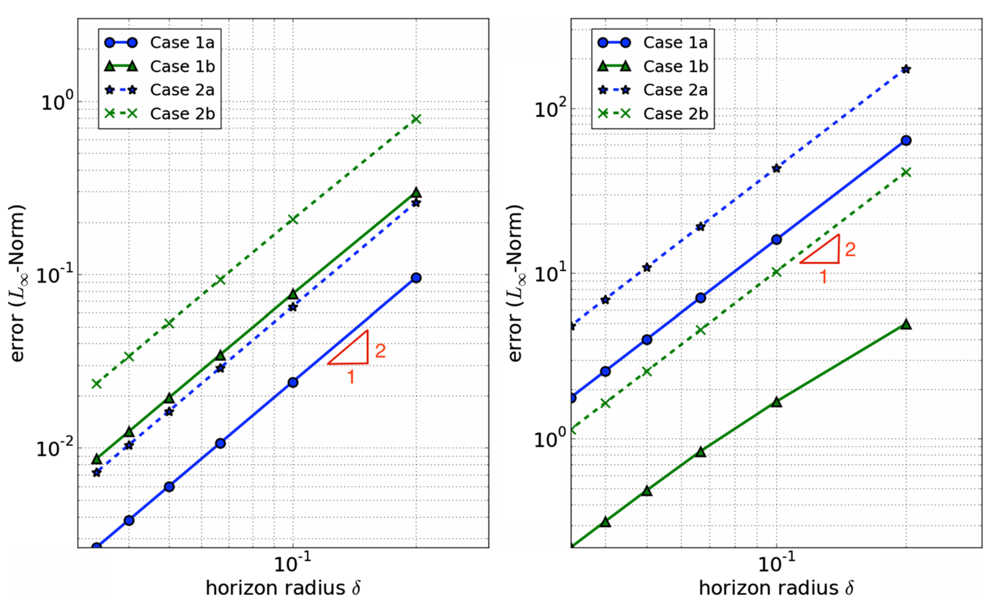

Fig. 6 L_∞-norm of the error in the nonlocal deformation gradient (*left*) and stress divergence operator (*right*) for cases 1 and 2

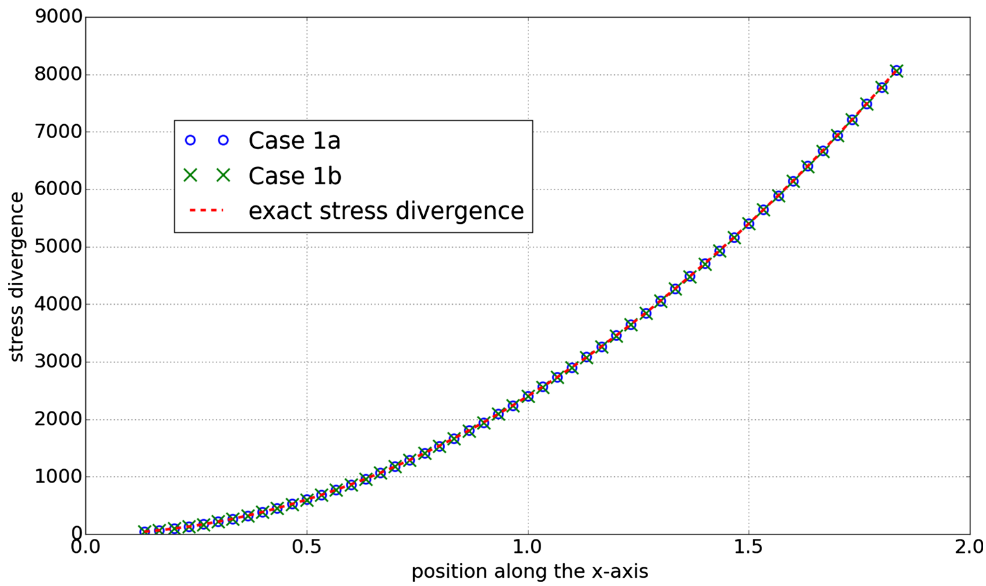

Fig. 7 Comparison of the nonlocal stress divergence to its local counterpart for case 1 using the smallest horizon radius

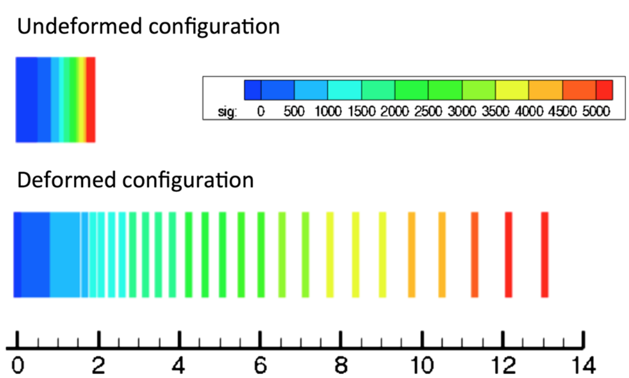

Fig. 8 Stress contours shown on the undeformed (*top*) and deformed (*bottom*) configuration

4.2 Numerical example II: uniaxial tension of a hyperelastic bar

In the second example, we employ both the total Lagrangian peridyunamics and the updated Lagrangian peridynamics formulations to simulate the uniaxial tension of a three-dimensional bar made of a hyperelastic material.

The dimension of the bar is set as $0.1 \times 0.1 \times 1.0$ (see Fig. 8a). The non-dimensional reduced unit is used, i.e we first choose a basic unit set of length, mass, and time $[L_0, m_0, t_0]$ as reference measure. The computed variables are related to real physical variables by the formula $L^* = L/L_0$; $v^* = (vt_0)/L_0$; $t^* = t/t_0$; $\rho^* = \rho/(m_0/L_0^3)$; $\sigma^* = \sigma/(m_0/(L_0 t_0^2)$, etc.

We performed a uniaxial tensile test with a total of 1075 peridynamics particles (Fig. 10). The column is modeled as a St. Venant-Kirchhoff elastic material,

$$\mathbf{S} = \lambda \mathrm{Tr}(\mathbf{E}) + 2\mu\mathbf{E}, \quad \text{and} \quad \mathbf{E} = \frac{1}{2}\left(\mathbf{F}^T\mathbf{F} - \mathbf{I}\right)$$

where $\mathbf{S}$ is the second Piola-Kirchhoff stress, and $\mathbf{E}$ is the Green-Lagrangian strain. The material parameters used in the numerical test are: $\lambda = 200$, and $\mu = 20$. Density of the column is set as $\rho_0 = 1.4$ such that the longitudinal wave speed is around 10.0. The bottom of the column is fixed with zero displacement in the vertical direction, and the top of the column is prescribed with a tensile traction $\tau_z = 14$.

For the total Lagrangian peridynamics, we employ the dynamics equations,

$$\begin{aligned}\rho_0 \ddot{\mathbf{u}}^A &= \sum_{B=1}^{N_{H_A}} \omega(\xi^{AB})\Big(\mathbf{P}(\mathbf{x}^B, t) - \mathbf{P}(\mathbf{x}^A, t)\Big)\\ &\quad \cdot \mathbf{K}^{-1}(\mathbf{X}^A)\boldsymbol{\xi}^{AB}\Delta V^B\\ &\quad + \mathbf{B}(\mathbf{X}^A, t), \quad A = 1, 2, \ldots, N,\\ \mathbf{F}_A &= \mathbf{N}(\mathbf{x}^A, \mathbf{X}^A)\mathbf{K}^{-1}(\mathbf{X}^A); \end{aligned} \tag{89}$$

and for the update Lagrangian peridynamics approach, we adopt the dynamics equations,

$$\begin{aligned}\rho_t^A \ddot{\mathbf{u}}^A &= \sum_{B=1}^{N_{H_A}} \omega(\xi^{AB})\Big(\boldsymbol{\sigma}(\mathbf{x}^B, t) - \boldsymbol{\sigma}(\mathbf{x}^A, t)\Big)\\ &\quad \cdot \mathbf{M}^{-1}(\mathbf{x}^A)\mathbf{Y}^{AB}\Delta V^B\\ &\quad + \mathbf{b}(\mathbf{X}^A, t), \quad A = 1, 2, \ldots, N;\\ \hat{\mathbf{F}}_A &= \mathbf{M}(\mathbf{x}^A)\mathbf{N}^{-T}(\mathbf{x}^A, \mathbf{X}^A). \end{aligned} \tag{90}$$

Figure 8 shows the original configuration and the deformed shape of the stretched bar. The deformed configuration sim-

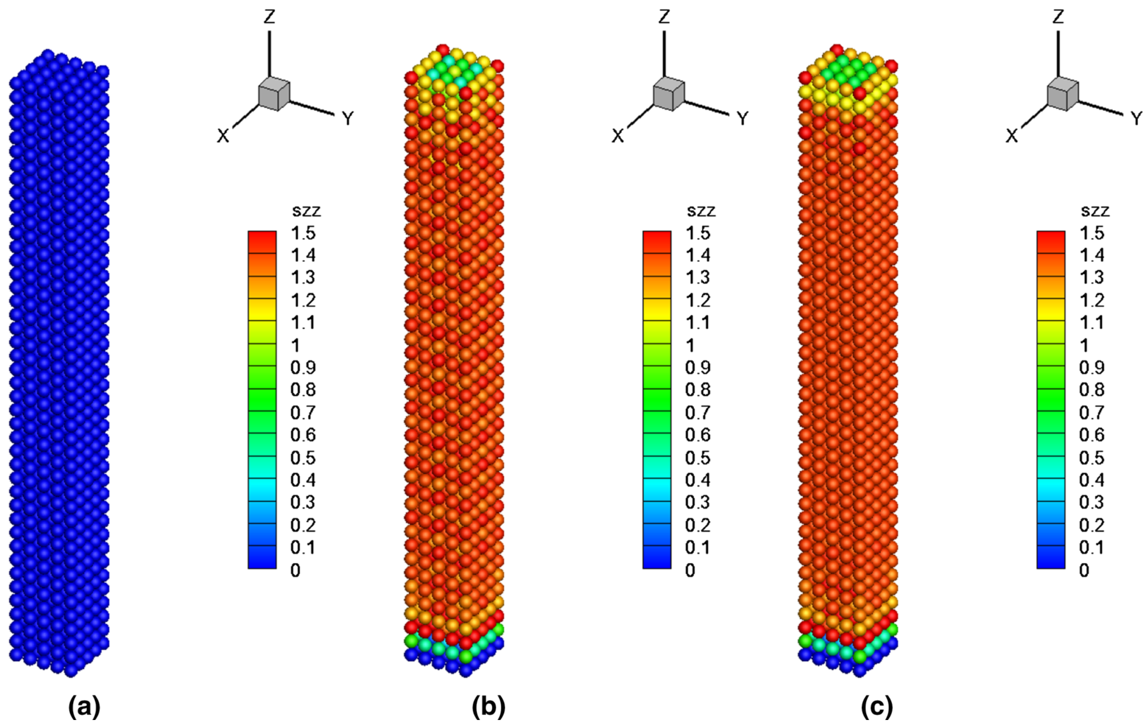

Fig. 9 Comparison of the total Lagrange approach and the updated Lagrange approach: **a** The initial configuration, **b** The total Lagrange calculation, and **c** the updated Lagrange calculation (The *color* contour is S_{33}). (Color figure online)

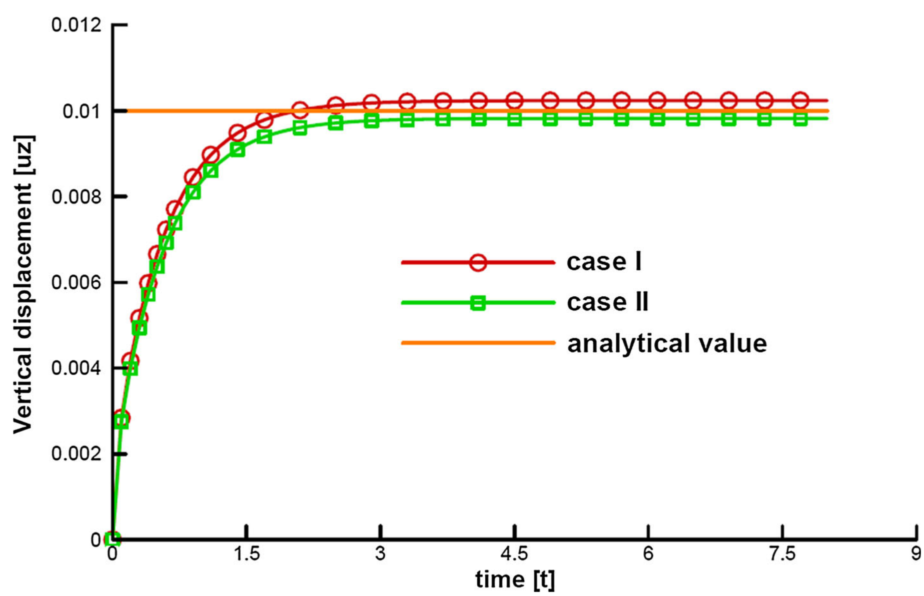

Fig. 10 Comparison of the time history of of elongation of an hyperelastic bar under uniaxial tension load via the total Lagrange and the update Lagrange computations. *Case I* Total Lagrange Method, and *Case II* Updated Lagrange Method

ulated by the total Lagrangian peridynamics and by the updated Lagrangian peridynamics are compared in Fig. 8b and c. The color contour is the second Piola-Kirchhoff stress component S_{zz}. The vertical displacements at the top column surface are measured and compared to the analytical result. In Fig. 9, we plot the time history of the top surface displacement for (a) analytical result for static solution (0.01), (b) the dynamics solution for the total Lagrangian peridynamics solution, which converges to 0.01024, and (c) the dynamics solution for the updated Lagrangian peridynamics solution, which converges to 0.00982. During the simulation, the adaptive dynamic relaxation (ADR) method ([17]) is used in order to get the static result. These results clearly indicate that both cases may converge to the corresponding analytical solution, as is being anticipated.

5 Conclusions

In this work, we study both the total Lagrangian and the updated Lagrangian formulations of stated-based peridynamics. It may be noted that these two formulations are related because the updated Lagrangian perdynamics formulation may be expressed in terms of the undeformed bonds mapped onto the spatial configuration, and whereas the total Lagrangian peridynamics may be expressed in terms of deformed bonds mapped into the referential configuration. Through these alternative formulations, we hope to motive a more broad use of peridynamics in nonlocal continuum mechanics that encompasses both solids and fluids.

The existing non-ordinary state-based peridynamics is a total Lagrangian formulation, the current total Lagrangian peridynamics formulation is only being formulated in terms of the undeformed bonds. Sometimes, the material constitutive relation may rely on deformed bonds, and this important issue has been ignored in the current peridynamics literature and we have discussed this problem in this paper.

Lastly, we have introduced various nonlocal differential operators in the context of nonlinear continuum mechanics, and we have discussed their connections to the local form of those differential operators in classical continuum mechanics. Most of these nonlocal differential operators are generalized from the form of the deformation gradient or force states of non-ordinary state-based peridynamics. Moreover, in this paper, we have introduced new force states and new representation of the deformation gradient based on the proposed nonlocal differential operators/It is shown both numerically and mathematically that these nonlocal deformation measures converge to their local counterparts as the radius of the horizon approaches zero.

Acknowledgments This work was supported by the ONR MURI Grant N00014-11-1-0691, which is gratefully acknowledged. Dr. Houfu Fan calculated the second numerical example.

References

1. Agwai A, Guven I, Madenci E (2011) Predicting crack propagation with peridynamics: a comparative study. Int J Fract 171(1):65–78
2. Bathe KJ (2008) Finite element method. Wiley, New York
3. Belytschko T, Liu WK, Moran B, Elkhodary K (2013) Nonlinear finite elements for continua and structures. Wiley, New York
4. Bessa MA, Foster JT, Belytschko T, Liu WK (2014) A meshfree unification: reproducing kernel peridynamics. Comput Mech 53:1251–1264
5. Bobaru F, Ha Y, Hu W (2012) Damage progression from impact in layered glass modeled with peridynamics. Open Eng 2(4):551–561
6. Bobaru F, Duangpanya M (2011) A peridynamic formulation for transient heat conduction in bodies with evolving discontinuities. J Comput Phys 231:2764–2785
7. Du Q, Gunzberger M, Lehoucq RB, Zhou K (2013) A nonlocal vector calculus, nonlocal volume-constrained problems, and nonlocal balance laws. Math Models Methods Appl Sci 23(3):493–540
8. Du Q, Gunzberger M, Lehoucq RB, Zhou K (2013) Analysis of the volume-constrained peridynamic Navier equation of linear elasticity. J Elast 113:193–217
9. Ericksen JL (2008) On the Cauchy-Born rule. Math Mech Solids 13(3–4):199–220
10. Finnis MW, Sinclair JE (1984) A simple empirical N-body potential for transition metals. Philos Mag A 50(1):45–55
11. Foster JT, Silling SA, Chen WW (2010) Viscoplasticity using peridynamics. Int J Numer Methods Eng 81(10):1242–1258
12. Garboczi EJ (1987) Cauchy relations for central-force random networks. Phys Rev B 36:2115–2120
13. Gerstle W, Sau N, Silling S (2007) Peridynamic modeling of concrete structures. Nucl Eng Des 237(12):1250–1258
14. Gunzburger M, Lehoucq RB (2010) A nonlocal vector calculus with application to nonlocal boundary value problems. Multiscale Model Simul 8(5):1581–1598
15. Ha YD, Bobaru F (2010) Studies of dynamic crack propagation and crack branching with peridynamics. Int J Fract 162(1–2):229–244
16. Holzapfel GA (2000) Nonlinear solid mechanics: a continuum approach for engineering. Wiley, West Sussex
17. Kilic B, Madenci E (2010) An adaptive dynamic relaxation method for quasi-static simulations using the peridynamic theory. Theor Appl Fract Mech 53:194–204
18. Li S, Ren B, Minaki H (2014) ‘Multiscale crystal defect dynamics: a dual-lattice process zone model. Philos Mag 94:1414–1450
19. Li S, Liu WK (2004) Meshfree particle methods. Springer, New York
20. Lipton R (2014) Dynamic brittle fracture as a small horizon limit of peridynamics. J Elast 117(1):21–50
21. Liu WK, Jun S, Li S, Adee J, Belytschko T (1995) Reproducing kernel particle methods for structural dynamics. Int J Numer Methods Eng 38(10):1655–1679
22. Madenci E, Oterkus E (2014) Peridynamic theory and its applications. Springer, New York
23. Mengesha T, Du Q (2014) Nonlocal constrained value problems for a linear peridynamic Navier equation. J Elast 115(1):27–51
24. Ren B, Houfu F, Bergel GL, Regueiro RA, Lai X, Li S (2014) A peridynamics-SPH coupling approach to simulate soil fragmentation induced by shock waves. Comput Mech 55:287–302
25. Silling SA (2000) Reformulation of elasticity theory for discontinuities and long-range forces. J Mech Phys Solids 48:175–209
26. Silling SA, Epton M, Weckner O, Xu J, Askari E (2007) Peridynamics states and constitutive modeling. J Elast 88:151–184
27. Silling SA, Bobaru F (2005) Peridynamics modeling of membranes and fibers. Int J Non-Linear Mech 40:395–409
28. Silling SA, Lehoucq RB (2008) Convergence of peridynamics to classical elasticity theory. J Elast 93:13–37
29. Silling SA, Lehoucq RB (2010) Peridynamic theory of solid mechanics. Adv Appl Mech 44(1):73–166
30. Tian X, Du Q (2013) Analysis and comparison of different approximations to nonlocal diffusion and linear peridynamic equations. SIAM J Numer Anal 51(6):3458–3482
31. Tupek MR, Radovitzky R (2014) An extended constitutive correspondence formulation of peridynamics based on nonlinear bond-strain measures. J Mech Phys Solids 65:82–92
32. Zeng X, Li S (2010) A multiscale cohesive zone model and simulations of fractures. Comput Methods Appl Mech Eng 199(9):547–556